Humanities and Social Sciences Communications

Article in Press

https://doi.org/10.1057/s41599-026-07775-y

The climate response prototype of dwellings built by indigenes: taking the temperate climate as an example

Received: 17 October 2024

Accepted: 20 May 2026

Cite this article as: Yang, L., Yuan, W., Liu, Y. *et al.* The climate response prototype of dwellings built by indigenes: taking the temperate climate as an example. *Humanit Soc Sci Commun* (2026). https://doi.org/10.1057/s41599-026-07775-y

Liu Yang, Weiqing Yuan, Yan Liu, Yuhao Qiao & Jiaping Liu

Manuscript for *Humanities & Social Sciences Communications*

The climate response prototype of dwellings built by indigenes: Taking the temperate climate as an example

ABSTRACT

Shielding humanity from climate change is a critical global issue. However, modern building design often relies on simplified environmental assumptions, leading to highly insulated and tightly sealed envelopes that maintain a constant indoor climate at the cost of substantial energy consumption. Conversely, indigenes worldwide have historically constructed dwellings that respond to local climate without relying on fossil energy. The present paper investigates the evolution of traditional dwellings built by indigenes over the past hundred years. By integrating climate potential analysis, architectural data mining from the literature, field measurements, and drawing upon the concept of prototype, the present study proposes a set of prototypical climate-responsive factors. The results indicate that shading of deep window openings, thermal inertia of the envelope, width-to-depth ratio, and thermal resistance of the envelope are key factors for dwelling performance in temperate climates. For traditional dwellings, these factors exhibit linear relationships with climate potential. Compared with modern building standards, these prototypical factors reflect a more comprehensive utilization of climatic resources rather than an approach based on environmental isolation. The findings highlight that even in temperate climate regions, shading, thermal mass, passive solar heating, and insulation remain essential, and the design should be guided by comprehensive performance indicators. This work provides quantitative design benchmarks for climate-responsive dwellings in temperate climates, and advances the study of the relationship between architecture and climate.

***Keywords*:** Traditional dwelling; Climate response; Indoor thermal environment; Temperate climate

Nomenclature

a_r	depth of the room (m)
b_r	opening of the room (m)
d	thickness of the wall where the window is located
D	thermal inertia of the wall (dimensionless)
l_c	Shading of Deep Window Openings (m)
q	surface heat flux ($W \cdot m^{-2}$)
$R_{w,g}$	South Orientation Window to Ground Ratio
$S_{w,a}$	south window area (m^2)
T	surface temperature (°C)

Abbreviations

TMY	typical meteorological year

1. Introduction

Essentially, buildings serve as shelters that create indoor microclimates with far smaller fluctuations than the outdoor environment. Consequently, buildings ought to be responsive to the regional climate of their location (Yang et al., 2024). From 2021 to 2024, extreme cold or heat events have caused widespread anxiety and fear across large parts of the global population (Lewandowski et al., 2024), as well as illness and even deaths (Ebi et al., 2021). In this context, protecting humanity from climate-related harm is a pressing global issue. However, simply increasing envelope thermal resistance and relying on the equipment to maintain a constant environment will consume a large amount of energy. For over 4000 years, Chinese traditional dwellings built by indigenes across diverse climates have maintained tolerable indoor thermal environments without relying on fossil fuels. Therefore, exploring and utilizing the climatic

response experience of traditional dwellings is of great significance for advancing climate-responsive design in modern buildings.

The inherent climate response of traditional dwellings has been widely documented and extensively studied (Chen et al., 2025). As early as the first century AD, long before the invention of physical environmental monitoring instruments, Marcus Vitruvius Pollio first identified strategies for improving the thermal performance of buildings. With the development of environmental testing techniques, the mechanisms by which traditional dwellings regulate the indoor and outdoor thermal environments have been examined with increasing precision. Numerous studies have established relationships between spaces, envelopes of traditional dwellings, and the local climate. For example, field measurements indicate that traditional bamboo-woven mud walls have a higher heat transfer coefficient than brick-concrete walls. As a result, rooms constructed with bamboo-woven mud walls dissipate heat more quickly at night, making them better suited to the hot and humid climates (Ding & Shu, 2024). Using morphological characterization methods, the linear relationship between roof slope and precipitation (Li et al., 2021), as well as correlations between courtyard types and ventilation efficiency (Zhong et al., 2023) have been revealed. If these climate response characteristics could be inherited, dwellings might evolve into more comfortable buildings. However, traditional construction techniques are often abandoned because they do not meet contemporary functional requirements, making it difficult to transmit their climate response knowledge (Ndude & Memela, 2024). This challenge underscores the need to explore effective ways of translating the climate response experience of traditional dwellings. Therefore, it is imperative to develop a climate response prototype that serves as a transferable and replicable reference, encapsulating the climate response experience of traditional dwellings.

The word “prototype” means “original or primitive pattern”, which serves as a reference framework for subsequent replication. Existing research on architectural prototypes has primarily focused on cultural and artistic dimensions of architecture (Ismail et al., 2024). In the field of heritage conservation, for example, scholars have developed 3D models of ancient buildings to better understand and transmit traditional construction techniques (Zarrabi & Valibeig, 2021). In contrast, a climate response prototype represents the simplest pattern reflecting the relationship between climate and architecture. It consists of a system of key factors capable of generating prototypical architectural forms. The prototype of Cave Dwellings has been proposed as one such example. The study revealed that cave dwellings regulate the mean radiant temperature through their massive envelopes and control indoor air velocity by carefully configuring spatial layouts and openings. Subsequent research further indicated that the thermal comfort range of Cave Dwelling occupants corresponds closely to the indoor thermal environment created by these architectural features (Yang, 2023). The studies have made significant contributions to the climate response theories of traditional dwellings in China. Moreover, a climate response prototype has been developed for extremely hot-dry and cold-dry climates, and new dwellings have been constructed accordingly. Field measurements indicate that the indoor environment of these buildings outperform those of other local dwellings (Yang et al., 2020). However, both the prototype of Cave Dwelling and the prototype for extremely hot-dry and cold-dry climates are highly climate-specific, limiting their applicability to other climatic regions.

Consequently, a significant amount of research has emerged worldwide focusing on the climate response of buildings in the temperate climate (Csa, Csb Csc, Cwa, Cwb, Cwc Cfa, Cfb, Cfc) of the Köppen classification (Beck et al., 2023). Early field studies in the Mediterranean region (Csa) indicate that the shape, facade width, envelope construction, window area, and roof

slope of traditional dwellings reflect strategies consistent with the bioclimatic design principles. A previous study suggested that 71.6% of apartments in Zurich (Cfb) demonstrate the greatest potential to reduce operational energy consumption through optimized spatial layout, compared to those in other climate types (Weber et al., 2024). Research in Cyprus (Csa) recommends courtyards configurations to mitigate higher summer temperatures (Üzümoğlu & Turkan, 2022), while monitoring of traditional courtyards in Seville (Csa) shows that the temperatures are 8.6 to 12.1 °C lower than outdoors in summer and 3.3 °C higher in winter (Mellado et al., 2023). Moreover, medium albedo materials (around 0.4) on walls are recommended to balance thermal performance, while high albedo materials (above 0.7) are preferred for pavements (Cabeza et al., 2022). Studies in Szentendre (Cfb) further demonstrate that it is necessary to adopt envelope thermal mass combined with ventilation to mitigate summer overheating in courtyards and indoor spaces (Cabeza et al., 2023). ASHRAE Standard 169–2021 classifies these regions as having the lowest heating and cooling demands compared with other climate zones (ASHRAE, 2021). European climatic zoning and bio-climatic design standards indicate that well-insulated envelopes and operable shading systems to prevent summer overheating, as well as the benefits of thermal mass and balanced ventilation with heat recovery (Bear I. & Nobatek., 2016). However, research on climate-responsive building design in China's corresponding climate zone has primarily focused on identifying suitable passive strategies. Previous studies on climate zoning have pointed out that in low-latitude, high-altitude regions of China (Cwa and Cwb), passive solar heating is appropriate, while thermal mass (with or without ventilation) and direct evaporative cooling are not suitable (Wang et al., 2021). When the building length-to-width ratio is optimized in combination with other design parameters, indoor heating demands in winter can be met primarily through solar gains (Meng et al., 2022), suggesting significant potential for passive solar heating in much of this

region. However, the Chinese Standard for Thermal Design of Civil Buildings (GB 50176-2016) recommends winter insulation measures in selected areas but generally does not emphasize summer heat prevention (Ministry of Housing et al., 2016).

In summary, systematically extracting the experience of climate-responsive prototypes of traditional dwellings in temperate climates is highly beneficial for promoting climate response design methodologies. However, previous research in the relevant regions in China has not yet established a comprehensive factor system to support such design applications. Therefore, the present study takes traditional dwellings in this region as a case and addresses the following questions: (1) What are the key factors for the temperate climate response of traditional dwellings? (2) What is the relationship between these factors and climate potential? (3) How effective are existing traditional dwellings in responding to the temperate climate? In the context of climate change, climate response design for buildings primarily aims to maintain an acceptable indoor thermal environment with minimal or no energy consumption. Accordingly, this study focuses specifically on the thermal performance, excluding lighting and acoustics from the scope of analysis. The study region is located between 93°-108° E longitude and 22°-30° N latitude, with an altitude between 400 and 3,500 meters above sea level. The average temperature ranges from 18 °C-25 °C in the hottest month (July) to 0 °C-13 °C in the coldest month (January), with an annual temperature range of approximately 13 °C. The annual total solar radiation reaches 1443 kWh/m^2. In brief, the region is characterized by cool summers, mild winters, moderate solar radiation, a large diurnal temperature range in January, and a moderate diurnal temperature range in July. In the present study, dwelling data were extracted from 6 types of traditional dwellings in the region. Through correlation analysis, 4 key factors for the prototype were identified, and their relationships with climate potential were clarified. Based on the established linear relationships,

factor ranges for typical cities and prototypical architecture were generated. Field measurements of typical dwellings further verified the influence of these 4 indicators and supported the predicted ranges of climate responsiveness.

2. Methodology

The research is based on the theory of climate response in buildings, with an integrated approach of theoretical analyses and field experiments. The study is structured into three phases: In "Phase 1: Dwelling classification and form data collection", 164 dwelling samples were collected and categorized. Computer-aided vector graphic processing tools were used to obtain data on building dimensions, structures, and other relevant parameters. After acquiring data for all types of dwellings, in "Phase 2: Prototypical factor identification and prototypical architectures construction", the values of all factors were first calculated based on the collected data. Subsequently, through correlation analysis, key factors were screened out as prototypical factors for climate response. Linear regression analysis was then conducted to obtain prediction intervals for these prototypical factors, thereby determining their value ranges in typical cities. Based on these ranges, prototypical architectures for typical cities were generated. Finally, in "Phase 3: Measuring climate response performance", on-site measurements were conducted to assess the climate response performance of the prototypical factors in typical cities. The process was conducted to confirm the effectiveness of the prototypical factors for climate response and their corresponding intervals. Figure 1 shows the flowchart of the paper.

2.1 Dwellings classification and form data collection

Dwellings classification involves categorizing a large number of samples from the study region based on their climate response strategies. The classification establishes a foundation for data quality control in subsequent data collection and analysis. In this study, 164 dwelling samples

were extracted from approximately 995,550 Chinese words of field research literature. Climate-response strategies in these dwellings to respond to the regional climate and regulate the indoor microclimate primarily encompass the combined effects of envelopes and spaces on indoor-outdoor heat transfer and indoor thermal environment distribution. Therefore, based on the envelope characteristics, the dwellings were categorized into three types: low thermal mass, high thermal mass, and hybrid (low and high thermal mass combined). In terms of space configurations, two types were identified: landed and lifted. By integrating envelopes and spaces characteristics, the 164 samples were classified into 6 types: landed dwellings with low mass envelopes, landed dwellings with hybrid envelopes, landed dwellings with high mass envelopes, lifted dwellings with low mass envelopes, lifted dwellings with hybrid envelopes, and lifted dwellings with high mass envelopes (Fig. 2). These dwellings were built between 1600 and 2000. The diverse dwelling types and the period of 400 years provide an adequate data foundation for the research.

The form data includes dimensional information for all building components involved in climate responsiveness. Due to the current lack of a relevant training dataset, it is not feasible to use machine learning methods to obtain data in bulk. In this study, the dimensional data for building components were manually obtained one by one using vector graphic tools. Therefore, this work was constrained by the completeness and clarity of the original architectural drawings, as well as time limitations. In the present paper, one example each from six types of dwellings built between 1600 and 1900, and one example each from six types built between 1900 and 2000, met strict criteria for climate-responsive component documentation (e.g., complete floor plans, material annotations). Therefore, there are only 12 dwelling samples used for subsequent analysis.

2.2 Prototypical factors and architectures

The climate response prototype consists of prototypical factors, which delineate the

characteristics of the climate response prototype. Previous studies have proposed numerous factors to depict building performance, comprehensively considering three modes of heat transfer. In this study, commonly used indicators in current standards or factors exhibiting variation with the distribution of climatic elements are selected to characterize the performance of a dwelling's envelope and space. Among them, spaces are examined from three perspectives: external form, indoor space, and operation. The Shape Factor is used to depict the thermal insulation and heat-gain prevention performance of the external form. The Width to Depth Ratio characterizes the ventilation and solar heating performance of the indoor space. Thermal Inertia represents the heat storage capacity of the envelope, while Thermal Resistance and Window to Wall Ratio depict its insulation performance. Additionally, it is observed that factors such as roof slope, height of the ground floor space, window area facing different directions, eaves length, window opening depth, and functional distribution across different indoor floors vary with the distribution of climatic elements in this region. Therefore, to provide a more comprehensive assessment of climate responsiveness in this region, these factors are incorporated into the analysis. Roof Slope reflects the roof's capacity to receive solar radiation. The Height Difference Between Indoor and Outdoor characterizes the ventilation performance of the ground floor. The South Orientation Window to Ground Ratio represents the performance of solar energy utilization by the south-facing envelope. The Window Area of Summer Prevailing Wind Direction depicts the envelope's performance in ventilation and cooling during summer. Eave Shading characterizes the envelope's performance in reducing solar radiant heat gain outside the window opening. Shading of Deep Window Openings depicts the envelope's performance in mitigating solar radiant heat gain entering the window opening. Finally, the Ratio of Living Area Percentages Between Floors 1 & 2 represents the performance of the operation in responding to the indoor thermal environment distribution

caused by solar radiation. Thus, 12 factors are selected (Fig. 3).

The factors were calculated using the dwelling sample form data collected during Phase 1 of the statistical process. To eliminate potential bias arising from the unequal proportional representation of different dwelling types, the samples were balanced across categories. Specifically, one example of each of the six types of buildings constructed between 1600 and 1900, and one example of each of the six types of buildings constructed between 1900 and 2000, were randomly selected, totaling 12 building samples with complete information for factor calculation. The specific calculation methods for the factors are as follows:

The Window to Wall Ratio, Thermal Resistance, and Thermal Inertia of the Envelope were calculated according to previous research (Ministry of Housing et al., 2016). The Window to Wall Ratio can be calculated as:

$$R_{w,w} = \frac{S_w}{S_f} \tag{1}$$

where $R_{w,w}$ is the Window to Wall Ratio; S_f is the area of a single facade of a building (m^2); S_w is the total area of door and window openings on that facade (m^2).

The Thermal Resistance of the Envelope can be calculated as:

$$r = r_1 + r_2 + ... + r_n \tag{2}$$

where r is the thermal resistance of a flat envelope wall composed of multiple layers of homogeneous materials ($m^2 \cdot K/W$); $r_1, r_2 \ldots\ldots r_n$ is the thermal resistance of each layer of material ($m^2 \cdot K/W$), which can be calculated as:

$$r_n = \frac{\delta}{\lambda} \tag{3}$$

where r_n is the thermal resistance of each layer of material ($m^2 \cdot K/W$); δ is the thickness of the material layer (m); λ is the thermal conductivity of the material [W/(m·K)], with values taken

as 0.79 W/(m·K) for fired clay bricks, 0.14 W/(m·K) for wood, 0.93 W/(m·K) for rammed earth, and 1.16 W/(m·K) for stone, according to reference (Ministry of Housing et al., 2016).

The Thermal Inertia Index of the Envelope can be calculated as:

$$D = D_1 + D_2 + ... + D_n \tag{4}$$

where D is the thermal inertia index of a flat envelope wall composed of multiple layers of homogeneous materials, dimensionless; D_1, D_2 …… D_n is the thermal inertia index of each layer of material, dimensionless, which can be calculated as:

$$D_n = r_n \cdot s_n \tag{5}$$

where D_n is the thermal inertia index of each layer of material, dimensionless; r_n is the thermal resistance of each layer for the material (m^2·K/W); S_n is the coefficient of heat accumulation for the material [W/(m^2·K)], with values taken as 10.30 W/(m^2·K) for fired clay bricks, 3.85 W/(m^2·K) for wood, 11.03 W/(m^2·K) for rammed earth, and 12.56 W/(m^2·K) for stone, according to reference (Ministry of Housing et al., 2016).

The calculation methods for the South Orientation Window to Ground Ratio, Eave Shading, and Shading of Deep Window Openings are proposed for traditional dwellings. The South Orientation Window to Ground Ratio can be calculated as:

$$R_{w,g} = \frac{S_{w,a}}{b_r \cdot a_r} \tag{6}$$

where $R_{w,g}$ is the South Orientation Window to Ground Ratio; $S_{w,a}$ is the south window area (m^2); b_r is the opening of the room (m); a_r is the depth of the room (m).

The Eave Shading is defined as the vertical distance extending from the outermost point of the eaves to the exterior surface of the wall. The comprehensive shading capacity is described in terms of the distance spanning from the exterior surface of the window to the outer facade of the

wall. In most cases, this distance is approximately equal to half of the thickness of the exterior wall. Accordingly, the Shading of Deep Window Openings can be calculated as:

$$l_c = \frac{d}{2} \tag{7}$$

where l_c is the Shading of Deep Window Openings (m); d is the thickness of the wall where the window is located (m).

After calculating the factors, the present study separately examined the correlation between each indicator of two groups of dwellings constructed in different decades and the effective hours of climate response strategies. The study employs Pearson correlation analysis to systematically investigate the correlation between the factors and the effective hours of climate response strategies. Effective hours refer to the periods during which passive design strategies, such as shading and ventilation, can maintain indoor thermal comfort without the use of active energy systems. This metric is derived from meteorological data and human thermal comfort criteria, and serves as a key indicator of the applicability of passive design strategies under different seasonal and weather conditions. The meteorological data utilized in this study were the TMY statistics (Yang, 2024) of the station where the traditional dwellings were located. The effective hours were calculated by Givoni's bioclimatic chart and the ASHRAE Handbook of Fundamentals Comfort Model (ASHRAE, 2020). The specific procedure for calculating the effective hours is as follows:

(1) Hourly dry-bulb temperature and relative humidity data were extracted from the TMY dataset. Each hourly data point (temperature–humidity pair) was plotted on Givoni's bioclimatic chart.

(2) According to the zoning principles of Givoni's chart, each hourly data point was classified into specific thermal response zones (e.g., direct comfort, sun shading), which are defined according to experimentally derived comfort boundaries with different passive design strategies.

(3) The ASHRAE adaptive comfort model was applied to define the indoor direct comfort zone, and hours whose outdoor conditions could be shifted into it through passive strategies indicated by Givoni's zones were identified as effective hours.

Factors of 6 traditional dwellings built in 1600-1900 with Pearson correlation coefficients greater than 0.9 with the effective hours were selected as prototypical factors for climate response. Linear regression analysis was then conducted to obtain prediction intervals for these prototypical factors, thereby determining their value ranges in typical cities. Based on these ranges, prototypical architectures for typical cities were generated.

2.3 Measuring climate response performance

Phase 2 identified 4 prototypical factors for climate response. To examine their performance in typical cities, environmental measurements were conducted in 4 representative existing dwellings. These dwellings were randomly selected from typical existing buildings to avoid any artificial manipulation of the validation results. The tested buildings were in good condition and met the daily living requirements of residents, ensuring that the measured data accurately reflected their climate response performance. The testing times, locations, and prototypical factors are shown in Table 1.

Figure 4 shows the instrument arrangement in the dwellings. Air temperature, heat flux, surface temperature, and solar radiation were obtained. Before testing the surface temperature and heat flow of the envelope, an infrared imager was used to image every measurement surface. Thus, avoid placing the test points on the thermal bridge (areas with significantly higher or lower temperatures in the infrared thermal images). In this way, the data obtained from the test points can represent the condition of the entire wall surface. The test instruments were fixed to the wall, ceiling, and floor surfaces.

All instruments employed for the tests complied with ISO Standard 7726-2002 (ISO, 2002). Detailed information regarding the instruments employed is shown in Table 2. All instruments were used to record data for 24 hours each day during the test period with a recording interval of 10 min.

The solar heat gain is calculated by summing up the radiation intensities measured using a solar radiometer. The heat transfer through the wall is obtained by cumulative calculation using a heat flux density meter.

3. Results

3.1 Prototypical factors

The correlation analysis of dwelling factors constructed between 1600 and 1900 identified key factors in Chinese dwellings that are adaptive to temperate climates, serving as prototypical factors for climate response. The results of the correlation analysis for dwellings built between 1900 and 2000 demonstrated the evolutionary trends of these factors.

3.1.1 Dwellings from 1600 to 1900

In Fig. 5, the correlation coefficients between the Shading of Deep Window Openings, Thermal Inertia of the Envelope, Width to Depth Ratio, Thermal Resistance of the Envelope, and the climate response strategies are above 0.9. The Shading of Deep Window Openings is highly positively correlated with the effective hours of Sun Shading of Windows ($R^2 = 0.99$), and a strong negative correlation with the effective hours of Passive Solar Direct Gain Low Mass ($R^2 = –0.81$). The results indicate that even in temperate climate regions, adjusting the depth of the window openings is an important way of regulating the amount of solar radiation heat gain. The Thermal Inertia of the Envelope is highly correlated with High Thermal Mass Night Flushed ($R^2 = 0.96$), indicating that dwellings in temperate climate regions enhance the thermal inertia of the envelope

for heat storage with ventilation during summer.

The Width to Depth Ratio and Thermal Resistance of External Walls are negatively correlated with the effective hours of cooling strategies and highly positively correlated with the effective hours of heat preservation and heating passive strategies. The correlation coefficient between the Width to Depth Ratio and effective hours of ventilation and cooling was -0.63, and the correlation coefficient with effective hours of Passive Solar Direct Gain Low Mass was 0.94. Unlike buildings in other climates that increase the Width to Depth Ratio to promote ventilation, traditional dwellings in temperate climates increase the Width to Depth Ratio to provide more solar gain for rooms. Similarly, the Thermal Resistance of the Envelope exhibits a correlation coefficient of 0.75 with the effective hours of Internal Heat Gain, and an even stronger correlation (0.98) with the effective hours of Passive Solar Direct Gain Low Mass. The results indicate that in temperate climates, increasing the thermal resistance of the external walls is not a way of preventing heat gain in summer, but a way of keeping heat in winter in dwellings from 1600 to 1900.

Other factors with correlations below 0.9 are considered not to be key factors in the dwelling's response to temperate climates. Therefore, the study has screened out the key factors as the prototypical factors for climate response. They are the Width to Depth Ratio, Thermal Inertia of the Envelope, Thermal Resistance of the Envelope, and Shading of Deep Window Openings.

3.1.2 Dwellings from 1900 to 2000

As shown in Fig. 6, the correlation coefficients between the factors of dwellings built between 1900 and 2000 and the effective hours of climate response strategies are all less than 0.9. Even the correlation coefficients between prototypical factors for climate response and the effective hours of climate response strategies decreased. The correlation between the Thermal Resistance of the Envelope and the effective hours of Internal Heat Gain decreased to 0.53. The correlation between

the other three prototypical factors and the effective hours changed from negative to positive. The Shading of Deep Window Openings exhibits a weakly negative correlation with the effective hours of Sun Shading of Windows, with a correlation coefficient of -0.47, representing a 142% change in direction and magnitude. The correlation between the Width to Depth Ratio and the effective hours of Passive Solar Direct Gain Low Mass decreased to -0.42. The rate of change is 145%. Moreover, the correlation between the Width to Depth Ratio and the effective hours of Natural Ventilation Cooling changed from negative to positive, with a rate of change of 145%. The correlation between the Thermal Inertia of the Envelope and High Thermal Mass Night Flushed decreased to -0.27. The rate of change is 128%.

3.2 Prototypical architecture

3.2.1 Linear regression for prototypical factors

Linear regression analyses were conducted between the 4 climate response prototypical factors and the effective hours of the corresponding climate response strategies, yielding the following results as depicted in Figures 7-10. The architectural models shown in these figures are based on data samples covering 6 building types.

Figure 7 demonstrates a strong linear relationship between the effective hours of Sun Shading of Windows and the Shading of Deep Window Openings. The data points lie within the 95% confidence interval, indicating a high level of certainty in their position relative to the fitted line. The Shading of Deep Window Openings increases as the effective hours of Sun Shading of Windows augment, with a slope of 5.26. The intercept of -0.1, indicates that when the effective hours of Sun Shading of Windows are 0, the minimum value of the Shading of Deep Window Openings is -0.1. However, since the Shading of Deep Window Openings must be greater than 0, the minimum value of the Shading of Deep Window Openings is also greater than 0. The

coefficient of determination (R^2) for this linear fit is 0.99, indicating an excellent fit between the Shading of Deep Window Openings and the fitted line. Thus, the relationship between the effective hours of Sun Shading of Windows and Shading of Deep Window Openings can be reliably described by this linear regression model.

Figure 8 demonstrates a strong linear relationship between the effective hours of High Thermal Mass Night Flushed and the Thermal Inertia of the Envelope. The data points fall within a 95% confidence interval, indicating a high degree of reliability in the fitted line. The Thermal Inertia of the Envelope increases as the effective hours of High Thermal Mass Night Flushed augment, with a slope of 0.01. The intercept of 3.65 indicates that when the effective hours of High Thermal Mass Night Flushed are 0, the minimum value of the Thermal Inertia of the Envelope is 3.65. The coefficient of determination (R^2) for this linear fit is 0.96, indicating an excellent fit between the Thermal Inertia of the Envelope and the fitted line. Thus, the relationship between the effective hours of High Thermal Mass Night Flushed and Thermal Inertia of the Envelope can be reliably described by this linear regression model.

Figure 9 demonstrates a strong linear relationship between the Width to Depth Ratio and effective hours of Passive Solar Direct Gain with Low Mass. The data points fall within a 95% confidence interval, indicating a high degree of reliability in the fitted line. The Width to Depth Ratio increases as effective hours of Passive Solar Direct Gain with Low Mass augment, with a slope of 0.002. The intercept is -2.055, indicating that when the effective hours of Passive Solar Direct Gain with Low Mass are 0, the minimum value of the Width to Depth Ratio is -2.055. However, since the Width to Depth Ratio must be greater than 0, its actual minimum value must be greater than 0. The coefficient of determination (R^2) for this linear fit is 0.94, indicating an excellent fit between the Width to Depth Ratio and the fitted line. Thus, the relationship between

the Width to Depth Ratio and effective hours of Passive Solar Direct Gain with Low Mass can be reliably described by this linear regression model.

Figure 10 demonstrates a strong linear relationship between the Thermal Resistance of the Envelope and effective hours of Passive Solar Direct Gain with Low Mass. The data points fall within a 95% confidence interval, indicating a high degree of reliability in the fitted line. The Thermal Resistance of the Envelope increases as the effective hours of Passive Solar Direct Gain with Low Mass augment, with a slope of 7.84. The intercept is -0.08, which indicates that when the effective hours of Passive Solar Direct Gain with Low Mass are 0, the minimum value of the Thermal Resistance of the Envelope is -0.08. However, since the Thermal Resistance of the Envelope must be greater than 0, its actual minimum value must be greater than 0. The coefficient of determination (R^2) for this linear fit is 0.98, indicating an excellent fit between the Thermal Resistance of the Envelope and the fitted line. Thus, the relationship between the Thermal Resistance of the Envelope and effective hours of Passive Solar Direct Gain with Low Mass can be reliably described by this linear regression model.

3.2.2 Prediction interval for prototypical factors

Thus, if it is known the effective hours of climate response strategies for any city, the prediction intervals for the 4 climate response prototype factors can be derived based on the above linear relationships. As shown in Table 3, the predicted interval of prototype factors for typical cities was obtained. The prediction intervals for the Shading of Deep Window Openings for all cities varied from 0.02 to 0.56. The prediction intervals for the Thermal Inertia of the Envelope were above 2.13. The prediction intervals for the Width to Depth Ratio were below 1.73. The prediction intervals for the Thermal Resistance of the Envelope were below 1.08.

3.3 Measurement results

The following are the results of testing the climate response performance of the 4 factors of existing dwellings.

3.3.1 Shading of Deep Window Openings

The dwelling tested in Liupanshui serves as a typical example that meets the prediction interval for the Shading of Deep Window Openings. As illustrated in Fig. 11, the shading effectively reduces the solar heat gain through the window. The maximum solar heat gain outside the window occurs between 11:00 AM and 12:00 PM, reaching 102.0 kJ/m². In contrast, the peak value on the indoor windowsill was delayed by approximately two hours and reached only 58 kJ/m², corresponding to a 43% reduction in peak solar heat gain due to the shading. Solar exposure outside the window lasted from 9:00 to 20:00 (11 hours), whereas the deep window opening reduced the exposure period to 9:00–18:00, reducing the duration by 18.2%. Consequently, the total solar radiant heat gain throughout the day is reduced by 34%. The results indicate that the tested dwelling in a temperate climate emphasizes the use of window shading to decrease solar heat gain.

3.3.2 Thermal Inertia of the Envelope

The Thermal Inertia of the Envelope of the 4 existing dwellings tested all fell below the predicted range. Consequently, Fig. 12 presents the summer testing results of the dwelling in Guiyang, featuring envelopes with different levels of thermal inertia, demonstrating the significant role of envelope thermal inertia in responding to the local climate. The thermal inertia values for the roof, west wall, and north wall are 4.56, 4.33, and 2.97, respectively. By comparing the heat flux densities during heat transfer from each envelope to the interior, it is evident that envelopes with higher thermal inertia exhibit greater attenuation of heat flux density on their interior surfaces. During the testing period, the maximum heat flux from the exterior surface of the roof to the

interior was 193.9 W/m², whereas the corresponding value at the interior surface was only 16.5 W/m², representing a reduction of 91.5%. At the exterior surface of the north wall, the maximum heat flux from the exterior surface to the interior surface was 25.9 W/m², while the interior surface was 21.9 W/m², indicating a 15.4% reduction. The maximum heat flux from the exterior surface of the west wall to the interior was 169.3 W/m². The interior surface maintained a heat flux density greater than or equal to 0 W/m², throughout the testing period. The results suggested that an envelope with thermal inertia of 4.33 was sufficient to shield the interior from the heat of outdoor temperatures and western solar radiation.

However, despite the arrangement of envelopes with greater thermal inertia on the orientations exposed to stronger climatic heat gains, the indoor spaces remained overheated for most of the time. As shown in Fig. 12, the indoor air temperature and the interior surface temperatures of both the roof and the west wall consistently remained above 26 °C during the testing period. Only the interior surface of the north wall was below 26 °C from 2:00 AM to 8:00 AM the next day. This is attributed to the failure of the thermal inertia of the tested dwellings to meet the predicted range. The results demonstrate that a reasonable design of thermal inertia is crucial for dwellings in temperate climates.

3.3.3 Width to Depth Ratio

The dwelling measured in Kunming exemplifies a typical case that falls within the predicted range for the Width to Depth Ratio. Figure 13 illustrates the heat transfer through the interior wall surfaces of the dwelling during winter. During the testing period, the walls oriented along the width direction lost less heat to the outdoors compared to those oriented along the depth direction. Specifically, the average daily heat transfer into the interior for walls in the width direction was 300.3 kJ/m², while the heat transfer out to the exterior was 306.0 kJ/m², resulting in an average

daily heat loss of 5.7 kJ/m². In contrast, for walls in the depth direction, the average daily heat transfer into the interior was 278.8 kJ/m², and the heat transfer out to the exterior was 323.9 kJ/m², corresponding to a substantially higher daily heat loss of 45.1 kJ/m². Consequently, for dwellings in temperate climates, an appropriate Width to Depth Ratio can effectively reduce winter heat loss and improve the overall thermal insulation performance of dwellings.

3.3.4 Thermal Resistance of the Envelope

The thermal resistance of the measured dwelling in Kunming falls below the prediction interval, whereas that of the dwelling in Cangyuan exceeds the upper bound of prediction interval. Figure 14 illustrates the relationship between the temperature difference between the indoor center and the ceiling and the temperature difference between the indoor center and outdoors for the two measured dwellings. It is evident that the smaller the thermal resistance, the greater the influence of outdoor temperature on the temperature near the envelope, resulting in a larger indoor temperature difference. In Kunming, the indoor temperature difference undergoes drastic changes as the indoor-outdoor temperature difference increases, with a fitted line slope of 1.8. Conversely, in Cangyuan, the indoor temperature difference changes gently with increasing indoor-outdoor temperature difference, exhibiting a fitted line slope of only 0.1. Moreover, the proportion of cases in which the indoor center temperature exceeds the outdoor temperature in Cangyuan is significantly greater than that in Kunming. The absolute value of indoor temperature differences is also notably smaller in Cangyuan. The results indicate that a reasonable design of thermal resistance is crucial for maintaining a uniform environment in dwellings located in temperate climates.

4. Discussion

The current study analyzed the correlation between the factors of dwellings and the number

of effective hours of passive strategies obtained from climatic analysis, identifying 4 key factors in Chinese traditional dwellings that respond to temperate climates. The evolution of these factors was examined by comparing dwellings from different periods. Linear regression is employed to establish linear relationships between these 4 factors and the effective hours of passive strategies, yielding the value ranges of these factors in typical cities. Subsequently, experiments validate the significant impact of these 4 indicators on climate responsiveness.

For traditional dwellings built between 1600 to 1900, the correlation coefficients between the Shading of Deep Window Openings, Thermal Inertia of the Envelope, Width to Depth Ratio, Thermal Resistance of the Envelope and the effective hours of climate response strategies are above 0.9, as shown in Fig. 5. The Thermal Inertia of the Envelope is highly correlated with effective hours of High Thermal Mass Night Flushed, with a correlation coefficient of 0.96 in Fig. 5. The existing studies in Szentendre (classified as Cfb in the Köppen classification) indicate that it is necessary to adopt envelope thermal mass combined with ventilation to mitigate overheating in courtyards and indoors during summer (Cabeza et al., 2023). This demonstrates that, even in an era without climate analysis methods, traditional dwellings built by indigenes were already capable of utilizing the cooling effect of envelope thermal mass in response to local climatic conditions. As shown in Fig. 12, the thermal inertia values of the roof, west wall, and north wall are 4.56, 4.33, and 2.97, respectively. At the exterior surfaces of the roof, west wall, and north wall, the maximum inward heat flux was 193.9 W/m², 169.3 W/m², and 25.9 W/m², respectively. For the roof with the highest thermal inertia, the heat flux on the interior surface decreased by 91.5% compared to the exterior surface. The result clearly demonstrates that higher thermal inertia leads to a more pronounced attenuation of inward heat flux. However, due to the technological limitations at the time of construction, the structural load-bearing capacity of the building was constrained, making

it difficult to adopt envelopes with even higher thermal inertia. Consequently, the thermal inertia of the measured dwelling was below the predicted range. During the testing period, the indoor temperature and the interior surfaces of the envelope remained above 26 °C, as shown in Fig. 12, indicating overheating issues. In contrast to modern building standards, Chinese standards consider that summer heat protection is generally not necessary in this region (Ministry of Housing et al., 2016), while American standards classify it as having the lowest heating and cooling demands among climatic regions (ASHRAE, 2021). Only European standards recognize that thermal mass and nocturnal ventilation are beneficial (Bear & Nobatek, 2016). However, the present study confirms that in temperate regions, the high thermal inertia of the envelope plays a crucial role in mitigating summer overheating. The findings provide evidence that may contribute to refining and supplementing existing Chinese and international building standards.

In Fig. 5, the Width to Depth Ratio of rooms in traditional dwellings is highly correlated with the effective hours of Passive Solar Direct Gain in Low Mass, with a correlation coefficient of 0.94. According to previous studies, when the Length-to-Width Ratio of a building is optimized in combination with other design indicators, it can meet indoor heating demands solely through solar energy during winter in temperate climates (Meng et al., 2022). This suggests that the indigenous dwellings had already developed capable of utilizing solar energy for heating. Winter testing in Kunming (Fig. 13) further supports this finding. The average daily heat loss from the interior surface of walls facing the width direction was 5.7 kJ/m², whereas walls facing the depth direction exhibited a substantially higher heat loss of 45.1 kJ/m². A previous study indicated that 71.6% of apartments in Zurich (classified as Cfb in the Köppen classification) have the greatest potential to reduce operational energy consumption through optimizing indoor spatial layout, compared to apartments in other climate zones (Weber et al., 2024). However, current Chinese (Ministry of

Housing et al., 2016), American (ASHRAE, 2021), and European (Bear & Nobatek, 2016) building standards do not explicitly address the Width to Depth Ratio as a thermal performance indicator. The present study further revealed the reasons behind this phenomenon from the perspective of heat transfer and highlights the importance of this spatial parameter, which may contribute to supplementing existing Chinese and international building standards. In the region, walls facing the width direction or the depth direction experience significant differences in heat transfer, affected by intense solar radiation and smaller indoor-outdoor temperature differences. The mode of heat transfer is similar to that of dwellings located at higher latitudes and altitudes, such as those on the Qinghai-Tibet Plateau (Zhang et al., 2022).

Measured dwellings No. 3 and No. 4 both fall outside the predicted range for the Thermal Resistance of the Envelope: No. 3 is below the interval, whereas No. 4 exceeds it. This difference results from locally sourced materials, rammed earth with higher density and thermal conductivity in No. 3, and low-density, low-conductivity thatch in No. 4. Under similar structural constraints, No. 4 more readily achieves higher thermal resistance. Figure 14 illustrates that dwelling No. 3 exhibits indoor temperature differences of up to 14 °C, while No. 4 shows almost no variation, indicating that envelopes meeting or exceeding the predicted range provide more uniform indoor temperatures. Although Chinese (Ministry of Housing et al., 2016) and European (Bear & Nobatek, 2016) standards regulate envelope heat transfer coefficient, their limits assume mechanically conditioned buildings and do not reflect the year-round natural ventilation typical of this region. Based on field data from naturally ventilated traditional dwellings, this study offers empirical evidence to help refine current standards. Nevertheless, factors such as window-opening behavior and airtightness changes due to material aging may influence the results and require further study.

According to the correlation coefficients, Shading of Deep Window Openings, Thermal

Inertia of the Envelope, Width to Depth Ratio, and Thermal Resistance of the Envelope are identified as the prototypical factors of climate response. By comparing Fig. 5 and Fig. 6, the correlation between the factors and the effective hours of climate response strategies reveals substantial shifts. The correlation between Shading of Deep Window Openings and Sun Shading of Windows changed from positive to negative, with a rate of change of 142%. The correlation between Thermal Inertia of the Envelope and High Thermal Mass Night Flushed changed from positive to negative, with a rate of change of 128%. The correlation between the Width to Depth Ratio and the effective hours of Natural Ventilation Cooling changed from negative to positive, with a rate of change of 145%. The change indicates that dwellings built between 1900 and 2000 placed greater emphasis on ventilation rather than heat prevention. This is because, as household appliances gradually entered rural homes during this period, the focus of cooling dwellings in summer shifted towards quickly expelling internally generated heat. The correlation between the Thermal Resistance of the Envelope and the effective hours of Internal Heat Gain decreased by 56%. This is because, between 1900 and 2000, there was a significant improvement in the efficiency and stability of heating equipment such as Kangs (heated beds) and stoves in rural areas. In addition to traditional heating methods like Kangs and stoves, new heating devices such as electric blankets and local heating systems emerged. Against the backdrop of rapid development in cooling and heating technologies, residents neither reject new technologies nor abandon traditional designs. Instead, they adjusted both to adapt to new situations (Zhong et al., 2023). Furthermore, the quality of health, education (Li et al., 2024), safety, and convenience (Pan et al., 2024) became factors that residents valued more highly. Therefore, there are significant differences in the correlation between these factors and the effective hours of climate response strategies.

Based on the above statistical and experimental results, the prototypical factors for climate

response of traditional dwellings in the temperate climate region of China were determined. Compared to the design approach that relies on simplistic assumptions to create a constant environment (Tian et al., 2023) adopted in modern buildings, these prototypical factors have been tested and validated by residents themselves. Existing bioclimatic design frameworks used bioclimatic chart to calculate effective hours typically employ bioclimatic charts to calculate the effective hours of various climate regulation strategies in a given region, thereby evaluating their potential applicability (Wang et al., 2023). However, such methods do not directly provide specific architectural design parameters. In comparison, the range of values for these prototypical factors identified in this study for typical cities will provide direct and operable references for architectural design in the temperate climate region. Buildings designed accordingly will more closely resemble the slightly fluctuating indoor environment of traditional dwellings, which is beneficial for extending the duration of residents' comfort. Moreover, the indoor environment can stimulate occupants to regulate the thermal environment through behaviors (Carrapiço et al., 2022), which is beneficial for occupants' health and satisfaction (Wang et al., 2023; Klotz et al., 2019). Additionally, the paper provides insights for the preservation and inheritance of traditional direct and operable. Previous research on dwelling prototypes focused on morphology (Wang et al., 2025). However, because traditional buildings often fail to meet modern functional requirements, they are frequently demolished, leaving issues of preservation and inheritance unresolved. By translating traditional climate-responsive experience into quantifiable design parameters, this study helps bridge the gap between heritage conservation and contemporary architectural practice. Previous studies have shown that modern buildings designed with reference to traditional passive strategies can enhance climate adaptability and reduce heating and cooling energy consumption (Li et al., 2025). Nevertheless, appropriate and actionable design parameters have rarely been

proposed. The prototypical factors proposed in the study developed performance-based design approaches. The extraction method for climate response experience proposed in this study can be extended to other climatic regions. Therefore, although traditional dwellings need to be improved such as daylighting performance (Redondo, 2024), air quality, and other environmental conditions, their climate response experience is worth reinterpretation and application.

However, several limitations should be acknowledged. Due to the current lack of a relevant training dataset, it is not feasible to use machine learning methods to obtain data in bulk. The building materials and construction details were obtained from documented descriptions attached to the selected samples. As a result, the number of building samples used to provide data is relatively small. We acknowledge that this constraint reduces the generalizability of the correlation and regression results. Field measurements are also inevitably influenced by confounding factors, including occupant behavior, material aging and degradation, and site-specific contextual conditions. In addition, the present study does not consider the physical environment, such as the light and sound environment. Future work should aim to take the above factors into account for more in-depth research. In the future, a database should be established as a training set for studies involving larger sample sizes and broader geographic coverage, thereby improving the precision and general applicability of the findings. In addition, controlled laboratory experiments with carefully managed variables should be conducted to rigorously verify the climate-regulating effects of key architectural factors across different climatic regions.

5. Conclusions

In the study, we proposed a climate response prototype with a set of factors for Chinese traditional dwellings for temperate climates. The mathematical relationship between the

prototypical factors for climate response and effective hours of climate response strategies was established. The major findings are summarized as follows:

(1) Width to Depth Ratio, Thermal Inertia of the Envelope, Thermal Resistance of the Envelope, and Shading of Deep Window Openings are identified as the prototypical factors for climate response. For traditional dwellings, the correlation coefficients between the 4 factors and effective hours of passive strategies are above 0.9.

(2) In temperate regions, the utilization of envelope thermal mass to prevent overheating in summer cannot be overlooked. The thermal inertia of existing dwellings fell below the predicted interval, leading to overheating when indoor temperatures remained above 26 °C during the testing period. For the envelope with the highest measured thermal inertia, the heat flux on the interior surface decreased by 91.5% compared to the exterior surface.

(3) Non-climatic factors, including the widespread adoption of household appliances in rural homes and the improvement of heating equipment, influenced the prototypical factor evolution. The correlation between the 4 factors and the effective hours of climate response strategies changed over time, with a change rate ranging from 56% to 145%.

This paper identifies 4 prototypical factors from traditional dwellings built by indigenes, calling for modern building standards to consider a more comprehensive set of climate-responsive indicators, including heat storage, shading, and insulation in temperate climates. However, several limitations should be acknowledged. Due to time and resource constraints, the number of building samples included in the analysis was relatively limited. Future research should employ data mining

methods and expand the dataset to improve the robustness and generalizability of the findings. In addition, the present study does not address other aspects of the physical environment, such as the daylighting and acoustic conditions. In the future, work should focus on the influence of climate response factors on light and sound environments, providing a more comprehensive reference for architectural design.

Declaration of competing interest

The authors declare that they have no known competing financial interests or personal relationships that could have appeared to influence the work reported in this paper.

Data availability

Data will be made available on request.

References

ASHRAE. (2020). Thermal environmental conditions for human occupancy: ANSI/ASHRAE 55, *ASHRAE: Atlanta, GA, USA,* 2020.

ASHRAE. (2021). Climatic Data for Building Design Standards: ANSI/ASHREA Standard 169–2021, *ASHRAE: Atlanta, GA, USA,* 2021.

Bear I. & Nobatek. (2016). European climate zones and bio-climatic design requirements, Brussel: European Commission, 2016.

Beck et al. (2023). High-resolution (1 km) Köppen-Geiger maps for 1901–2099 based on constrained CMIP6 projections. *Scientific Data*, 10 (2023) 724. https://doi.org/10.1038/s41597-023-02549-6.

Cabeza et al. (2022). Albedo influence on the microclimate and thermal comfort of courtyards under Mediterranean hot summer climate conditions. *Sustainable Cities and Society*, 81 (2022) 103872. https://doi.org/10.1016/j.scs.2022.103872.

Carrapiço et al. (2022). Understanding thermal comfort in vernacular dwellings in Alentejo, Portugal: A mixed-methods adaptive comfort approach. *Building and Environment*, 217 (2022), 109084. https://doi.org/10.1016/j.buildenv.2022.109084.

Cabeza et al. (2023). Effect of thermal inertia and natural ventilation on user comfort in courtyards under warm summer conditions. *Building and Environment*, 228 (2023) 109812. https://doi.org/10.1016/j.buildenv.2022.109812.

Chen et al. (2025). Exploring the spatial distribution characteristics and formation mechanisms of Hakka folk settlements: a case study of Hakka traditional architecture in southeastern China. *Humanities and Social Sciences Communications*, 12 (2025), 380. https://doi.org/10.1057/s41599-025-04561-0.

Ding D. & Shu B. (2024). Thermal characteristics of dwellings with bamboo-woven mud walls in summer: A case study. *Journal of Building and Engineering*, 82 (2024), 108209. https://doi.org/10.1016/j.jobe.2023.108209.

Ebi et al. (2021). Hot weather and heat extremes: health risks. *The Lancet*, 398 (2021), 698-708. https://doi.org/10.1016/S0140-6736(21)01208-3.

ISO. (2002). Thermal environments specifications relating to appliances and methods for measuring physical characteristics of the environment, Standard International Organization for Standardization, *Geneva, Switzerland*, 2002.

Ismail et al. (2024). Traces of Turco-Persian influences in Malay woodcarving motifs on vernacular buildings in Terengganu. *Humanities and Social Sciences Communications*, 11 (2024), 1692. https://doi.org/10.1057/s41599-024-04173-0.

Klotz et al. (2019). Design behavior for sustainability. *Nature Sustainability*, 2 (2019) 1067-1069. https://doi.org/10.1038/s41893-019-0449-1.

Li et al. (2021). Change of extreme snow events shaped the roof of traditional Chinese architecture in the past millennium. *Science Advances*, 7 (2021), 1-8. https://doi.org/10.1126/sciadv.abh2601.

Li et al. (2024). Hesitant or determined? The influence of social and environmental factors on settlement decision making of rural in-migrants: evidence from Dali, China. *Humanities and Social Sciences Communications*, 11 (2024), 710. https://doi.org/10.1057/s41599-024-03188-x.

Lewandowski et al. (2024). Climate emotions, thoughts, and plans among US adolescents and young adults: a cross-sectional descriptive survey and analysis by political party identification and self-reported exposure to severe weather events. *The Lancet Planetary Health*, 8 (2024),

879–893. https://doi.org/10.1016/S2542-5196(24)00229-8.

Li et al. (2025). Passive design patterns for Hotan earth buildings under hot-arid climatic conditions of the Taklamakan Desert. *Energy and Buildings*, 349 (2025) 116546. https://doi.org/10.1016/j.enbuild.2025.116546.

Ministry of Housing et al. (2016). Code for Thermal Design of Civil Buildings (GB 50176-2016). *China Architecture and Building Press*, Beijing, China, 2016 (In Chinese).

Meng et al. (2022). A fast solar architecture design method towards zero heating energy: A SHF-SLR-based model and its parameters. *Energy*, 258 (2022) 124897. https://doi.org/10.1016/j.energy.2022.124897.

Mellado et al. (2023). Seasonal analysis of thermal comfort in Mediterranean social courtyards: A comparative study. *Journal of Building Engineering*, 78 (2023) 107756. https://doi.org/10.1016/j.jobe.2023.107756.

Ndude, A. & Memela S. (2024). Utilisation of rondavel space by amaXhosa people: a case of Mbhashe local municipality, Eastern Cape Province, South Africa, *Humanities and Social Sciences Communications*, 11 (2024), 1122. https://doi.org/10.1057/s41599-024-03649-3.

Pan et al. (2024). Community support as a driver for social integration in ex-situ poverty alleviation relocation communities: a case study in China. *Humanities and Social Sciences Communications*, 11 (2024), 1206. https://doi.org/10.1057/s41599-024-03650-w.

Redondo G. (2024). From the backyard to collective gardens in the “blue-courtyard”: Reversing the process of upgrading historic timber-framed courtyard buildings in Madrid. *Frontiers of Architectural Research*, 13 (2024) 265–283. https://doi.org/10.1016/j.foar.2023.12.004.

Tian et al. (2023). Energy saving retrofit of rural house based on the joint utilization of solar collector and attached sunspace. *Energy and Buildings*, 26 (2023), 1-9.

https://doi.org/10.1016/j.enbuild.2023.1135917.

Üzümoğlu M.D. & Turkan Z. (2022). Architectural characteristics of accommodation buildings within the context of sustainable ecotourism in Cyprus: evaluation and recommendations. *Humanities and Social Sciences Communications*, 9 (2022) 422. https://doi.org/10.1057/s41599-022-01443-7.

Wang et al. (2021). Applicability of passive design strategies in China promoted under global warming in past half century. *Building and Environment*, 195 (2021) 107777. https://doi.org/10.1016/j.buildenv.2021.107777.

Wang et al. (2023). Indoor thermal comfort evaluation of traditional dwellings in cold region of China: a case study in Guangfu Ancient City. *Energy and Buildings*, 288 (2023), 1-17. https://doi.org/10.1016/j.enbuild.2023.113028.

Wang et al. (2023). Can the ASHRAE Standard 169 zoning method be applied to country-level energy-efficient building design in China? *Building Simulation*, 16 (2023), 1041–1058. https://doi.org/10.1007/s12273-023-1017-1.

Weber et al. (2024). A hypergraph model shows the carbon reduction potential of effective space use in housing. *Nature Communications*, 15 (2024) 1-14. https://doi.org/10.1038/s41467-024-52506-z.

Wang et al. (2025). Study on the spatial relationships of traditional regional dwellings in Huizhou district. *npj Heritage Science*, 13 (2025), 238. https://doi.org/10.1038/s40494-025-01805-9.

Yang et al. (2020). Adaptive thermal comfort and climate responsive building design strategies in dry-hot and dry-cold areas: case study in Turpan, China. *Energy and Buildings*, 209 (2020). 1-16, https://doi.org/10.1016/j.enbuild.2019.109678.

Yang L. (2023). Mechanisms of climatically responsive building and principles of low-energy

building design, *Scientia Sinica Technologica*, 53 (2023) 1781–1794. https://doi.org/10.1360/SST-2023-0128 (In Chinese).

Yang et al. (2024). Toward interdisciplinary integration of architecture and climatology. *The Innovation Energy,* 1 (2024), 100054–2. https://doi.org/10.59717/j.xinn-energy.2024.100054.

Yang L. (2024). https://buildingdata.xauat.edu.cn/index.html. Accessed 25 Jun 2024.

Zarrabi M. & Valibeig N. (2021). 3D modelling of an Asbad (Persian windmill): a link between vernacular architecture and mechanical system with a focus on Nehbandan windmill, *Heritage Science*, 9 (2021) 108. https://doi.org/10.1186/s40494-021-00587-0.

Zhang et al. (2022). Method for dynamic thermal insulation design revealing almost real heat transfer characteristics of building envelopes in different Chinese regions. *Energy and Buildings*, 274 (2022) 112419. https://doi.org/10.1016/j.enbuild.2022.112419.

Zhong et al. (2023). Numerical investigations on natural ventilation in atria of China's southern Yangtze vernacular dwellings. *Sustainable Cities and Society*, 89 (2023), 1-18. https://doi.org/10.1016/j.scs.2022.104341.

Ethical approval

The study does not involve human participants or their data.

Informed consent

The study does not involve human participants or their data.

Author contributions

LY: Conceptualization, methodology, writing—review & editing, funding acquisition. WY:

Writing—original draft, visualization. YL: Formal analysis, validation. YQ: Writing—review & editing. JL: Investigation, data curation.

Figure captions

Table captions

Table 1
Basic information of tested dwellings

Dwellings	No. 1	No. 2	No. 3	No. 4
Time	Jul. 15-18, 2023	Aug. 3-10, 2024	Jan. 31, 2024 to Feb. 6, 2024	Jan. 6-9, 2013
Location	Liupanshui	Guiyang	Kunming	Cangyuan
Shading of Deep Window Openings	0.20 m	0.05 m	0.20 m	0.50 m
Thermal Inertia of the Envelope	4.33	3.43	4.10	0.81
Width to Depth Ratio	1.00	0.63	0.51	0.63
Thermal Resistance of the Envelope	0.34 m^2·K/W	0.72 m^2·K/W	0.34 m^2·K/W	1.70 m^2·K/W

Table 2
Detailed information of instruments

Description	Trade name	Parameter measured	Range	Accuracy
Digital temperature and humidity	T And D TR 72Ui	Air temperature	–20 °C-70 °C	±0.3 °C
		Relative humidity	10-95% RH	±3%

recorder				
Anemometer	Swema 3000	Air velocity	0.05-3 m/s	±0.03 m/s
Probe thermometer	Center® SE309	The surface temperature of the wall	–50 °C-50 °C	±0.05 °C
Probe thermometer with a 150 mm diameter black metal ball	Center® SE309	Globe temperature	–50 °C-50 °C	±0.5 °C

Table 3
Prototype architectures and prediction interval of the factors

Typical Cities	Prototype architectures	Shading of Deep Window Openings	Thermal Inertia of the Envelope	Width to Depth Ratio	Thermal Resistance of the Envelope
Gongshan	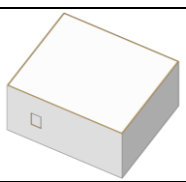	[0.02, 0.14]	[2.13, 6.11]	[0.60, 1.73]	[0.86, 1.08]
Fugong	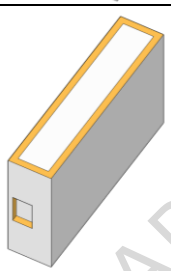	[0.26, 0.38]	[7.08, 11.79]	(0, 0.44]	[0.25, 0.62]
Kunming	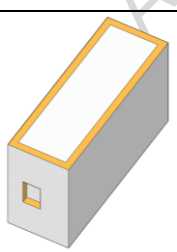	[0.32, 0.44]	[6.35, 10.64]	(0, 0.69]	[0.41, 0.72]
Guiyang	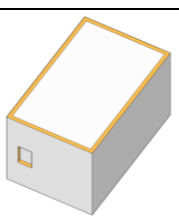	[0.21, 0.33]	[6.23, 10.48]	None	(0, 0.33]

Yongren	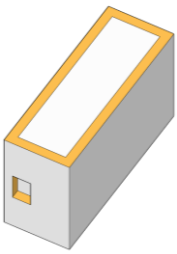	[0.41, 0.56]	[9.77, 16.69]	(0, 0.71]	[0.42, 0.73]
Liupanshui	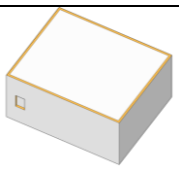	[0.16, 0.27]	[4.81, 8.62]	None	(0, 0.42]
Cangyuan	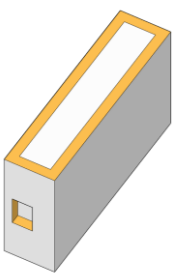	[0.41, 0.55]	[7.96, 13.27]	(0, 0.50]	[0.29, 0.64]

Phase 1: Dwelling classification and form data collection

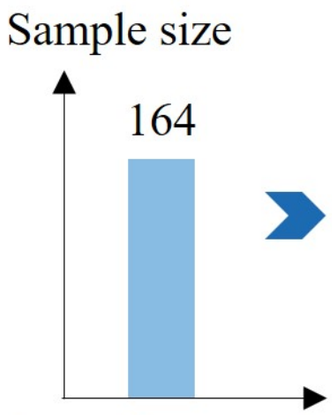

Dwelling samples

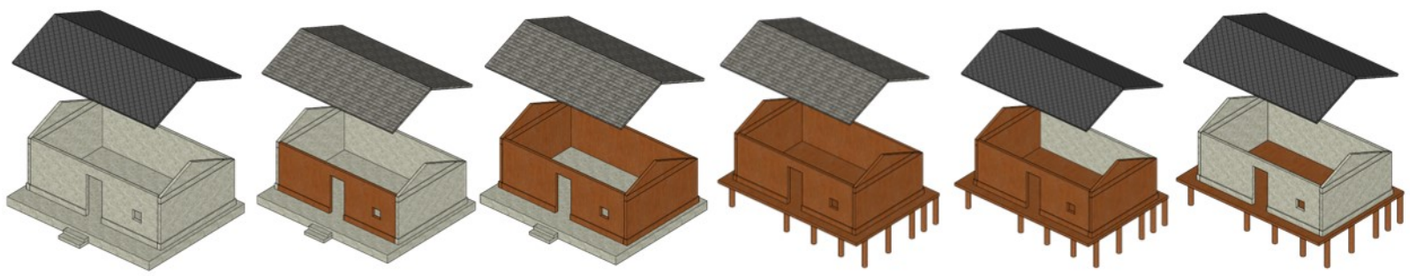

Classification of dwellings by spaces and envelopes

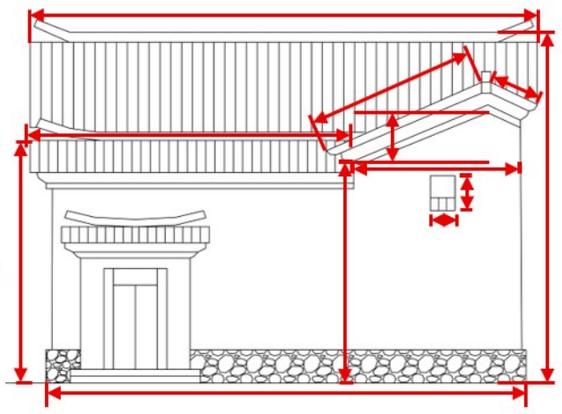

Data Collection (12 samples)

Phase 2: Prototypical factor identification and prototypical architecture construction

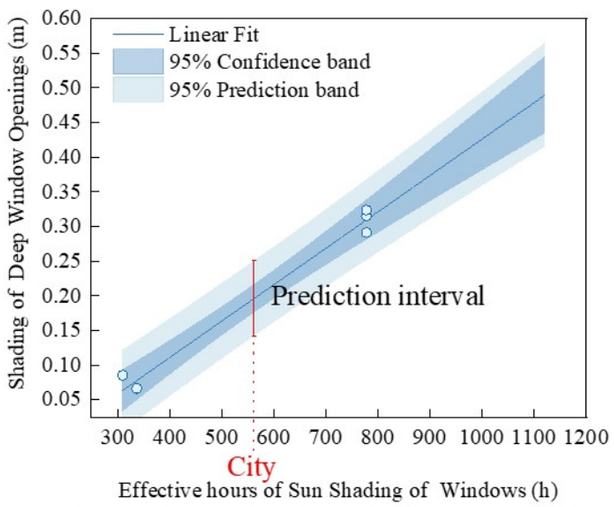

4 Prototypical factors prediction interval of typical cities (6 samples)

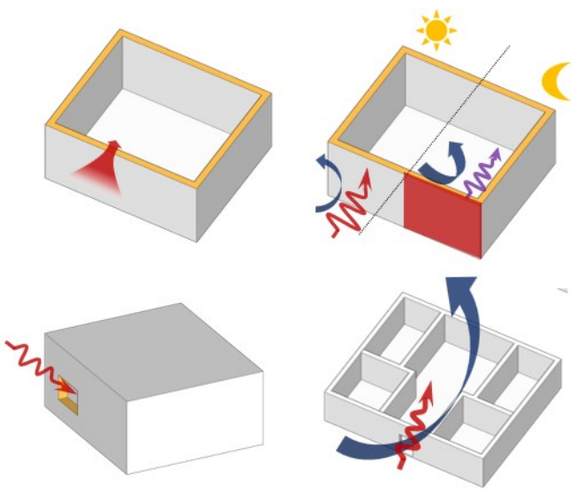

4 Prototypical factors (6 samples)

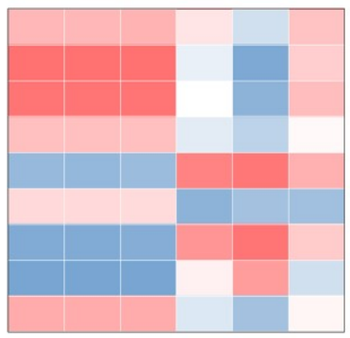

Screening and evolutionary analysis (12 samples)

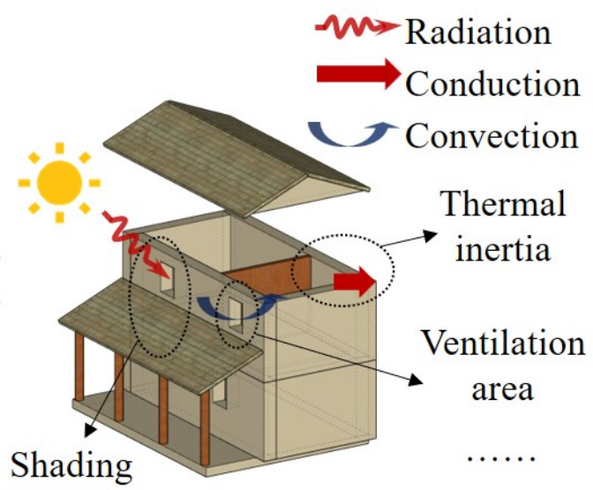

Factors calculation (12 samples)

Phase 3: Measuring climate response performance

Randomly select 4 dwellings in typical cities to test 4 prototypical factors

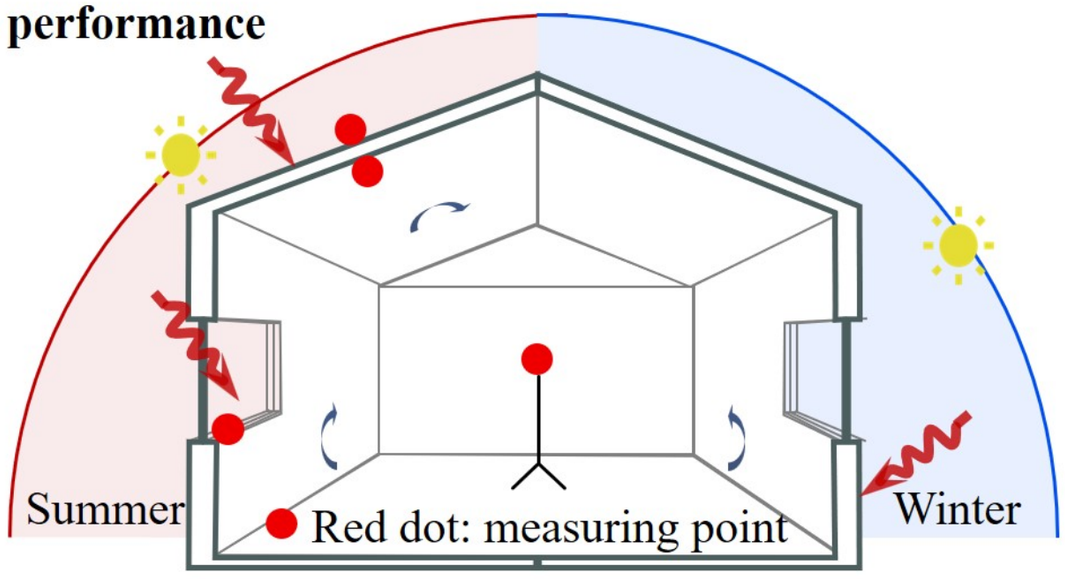

Multi-season, multi-point continuous measurement

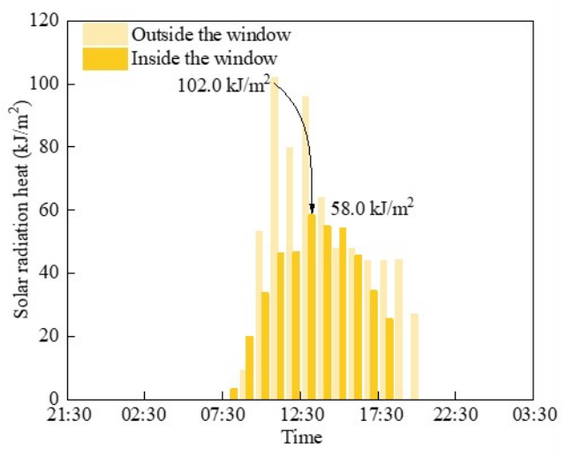

Effectiveness evaluation

Fig. 1 Flowchart of the study

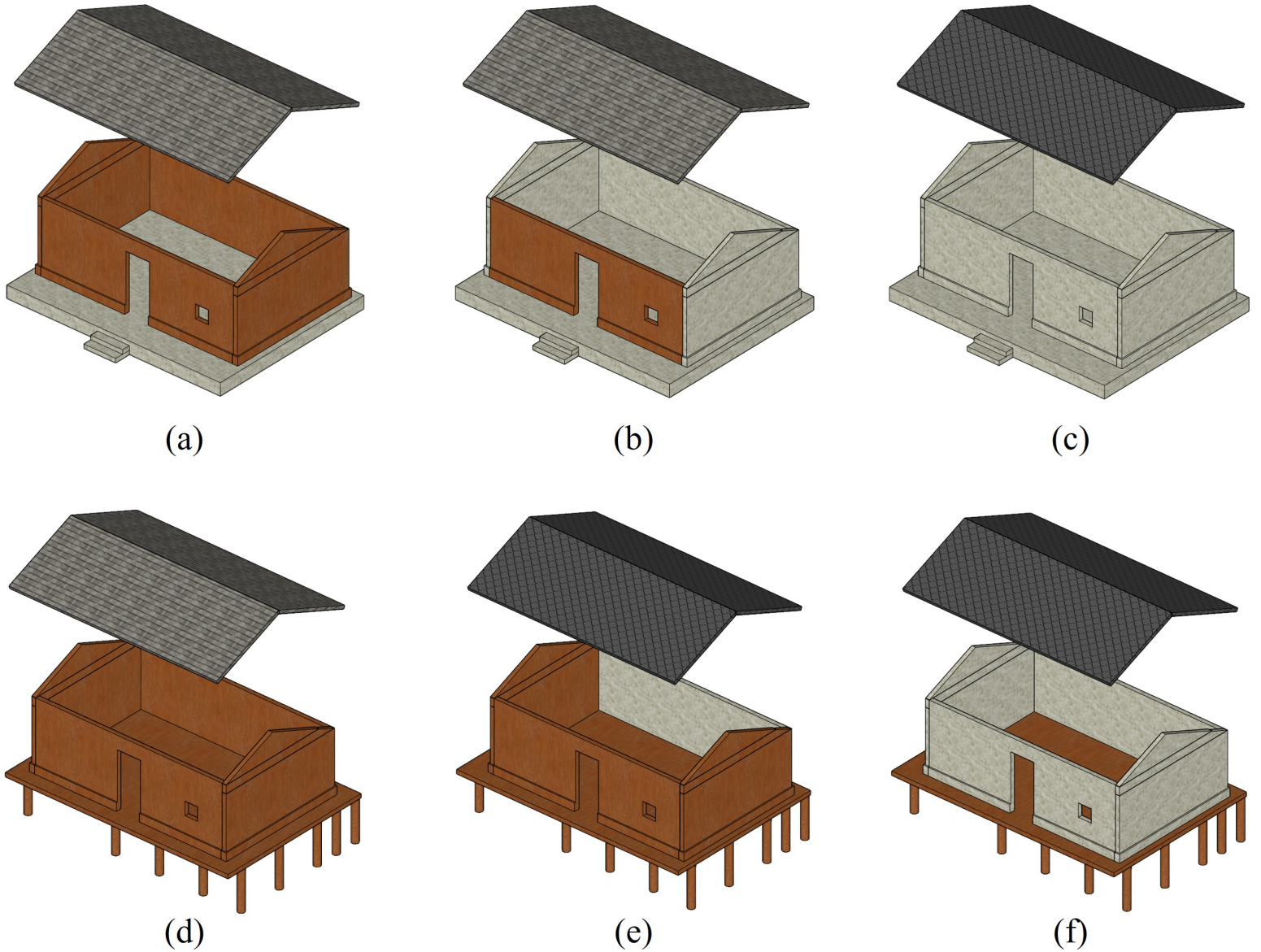

Fig. 2 Typical traditional dwellings in the temperate climate region of China: (a) landed dwellings with low mass envelopes, (b) landed dwellings with hybrid envelopes, (c) landed dwellings with high mass envelopes, (d) lifted dwellings with low mass envelopes, (e) lifted dwellings with hybrid envelopes, (f) lifted dwellings with high mass envelopes

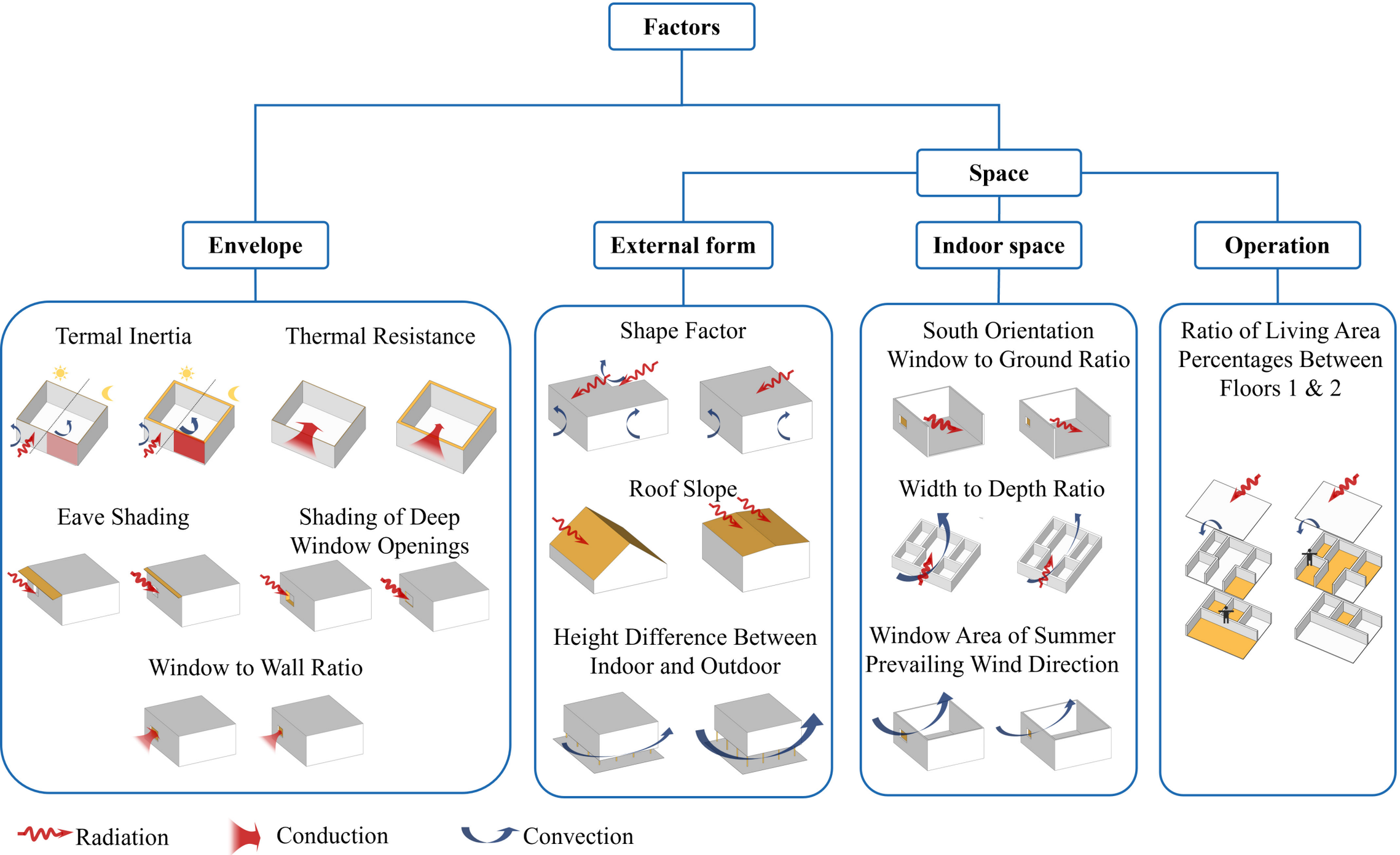

Fig. 3 Twelve factors to be tested

Dwelling No. 1

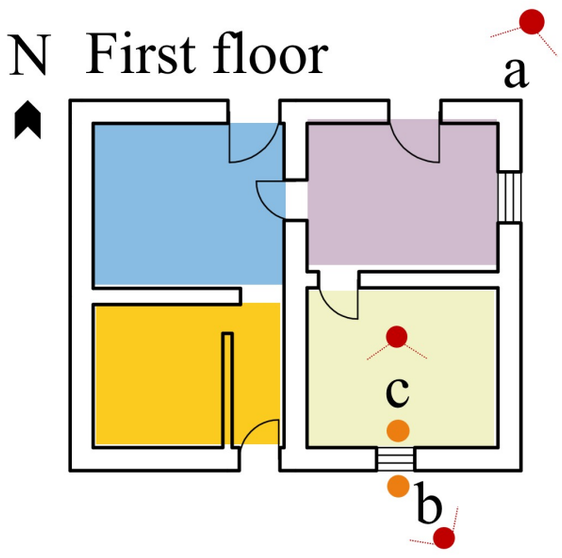

Dwelling No. 4

It has been a long time since testing (2013), and the sectional drawings have been lost.

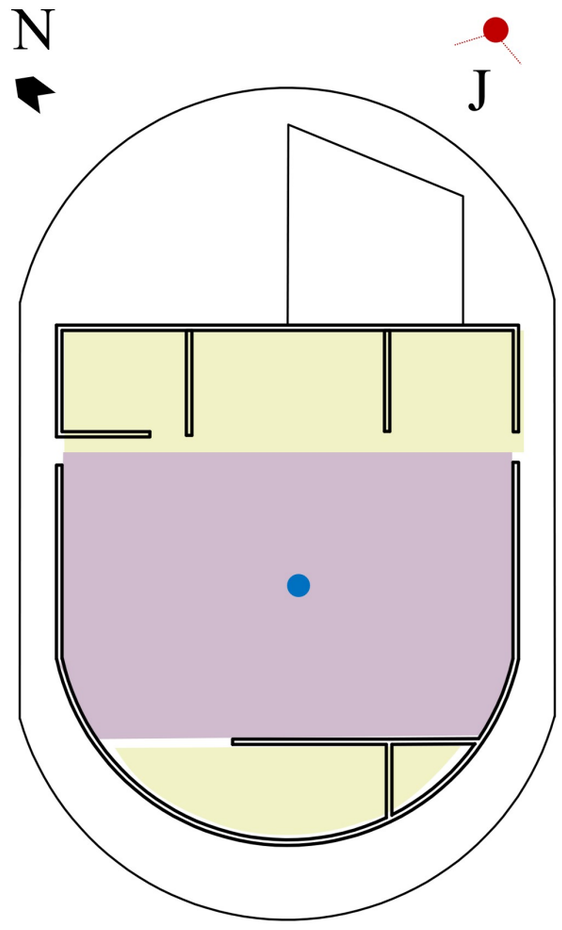

Dwelling No. 2

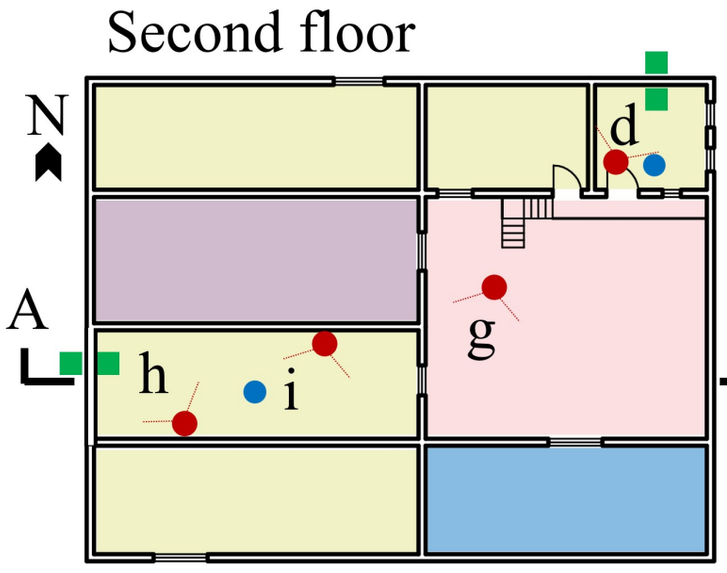

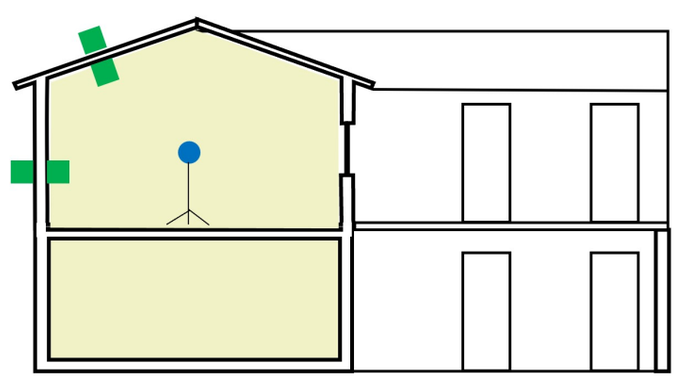

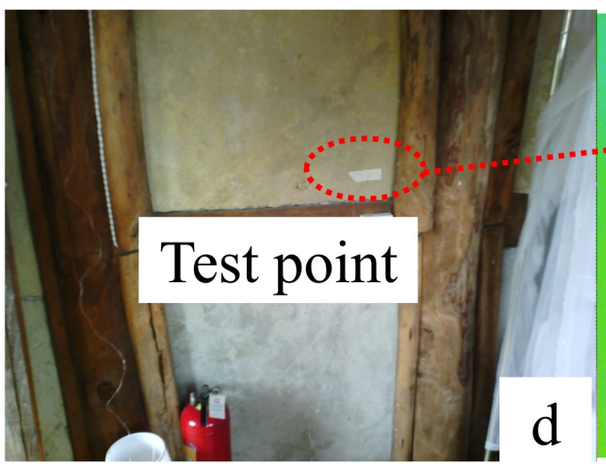

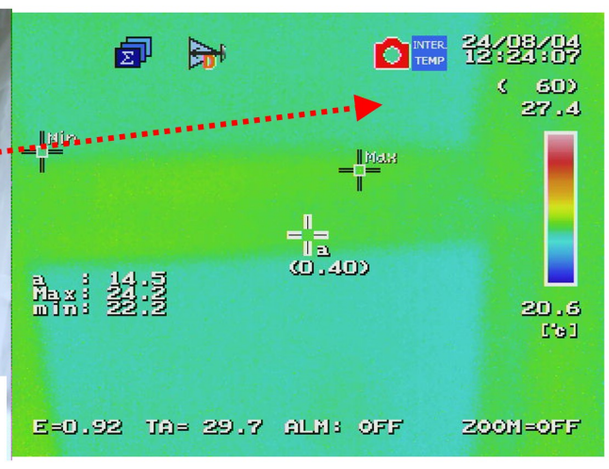

Infrared thermal image

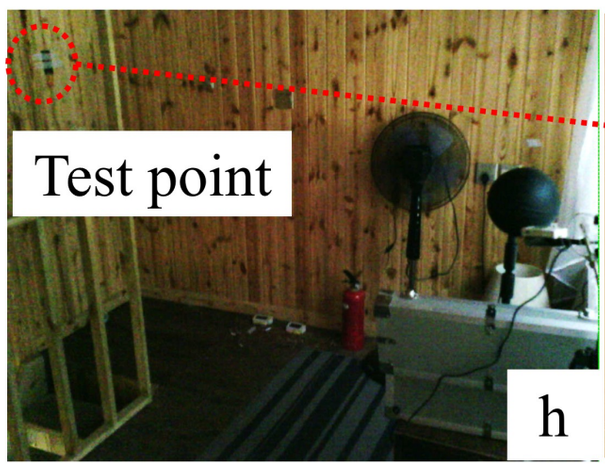

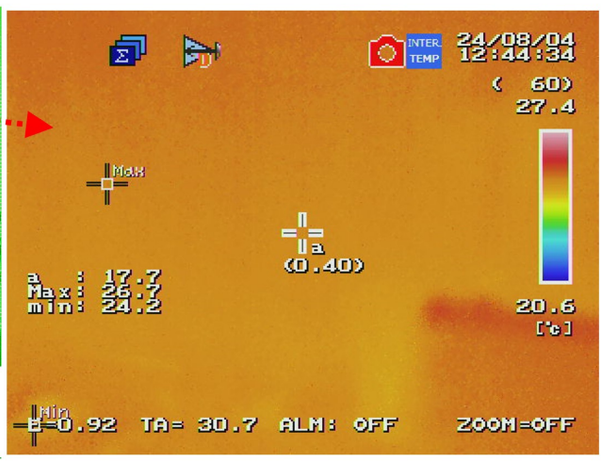

Infrared thermal image

Dwelling No. 3

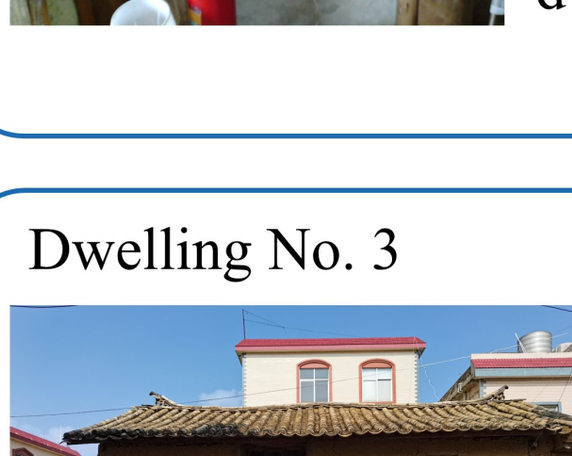

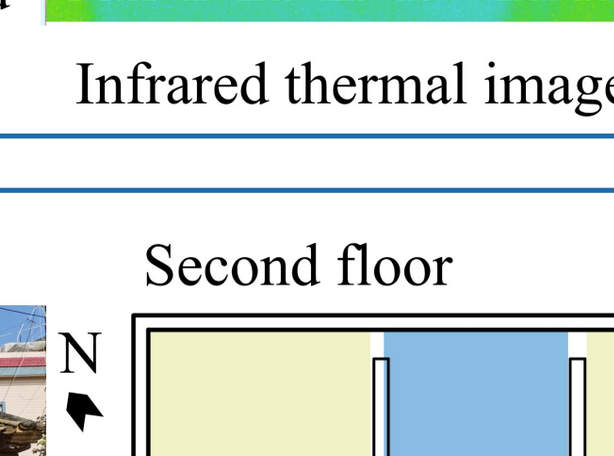

Infrared thermal image

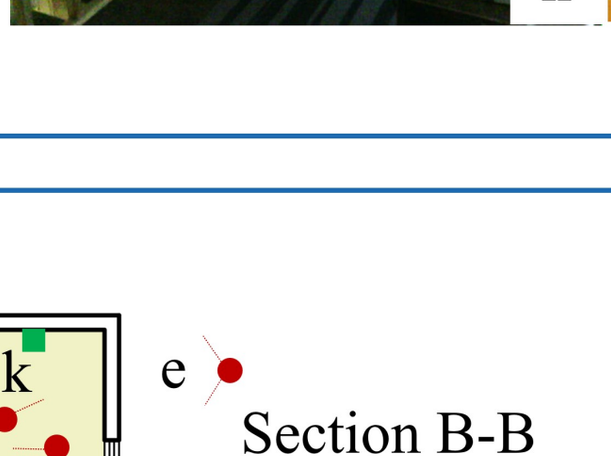

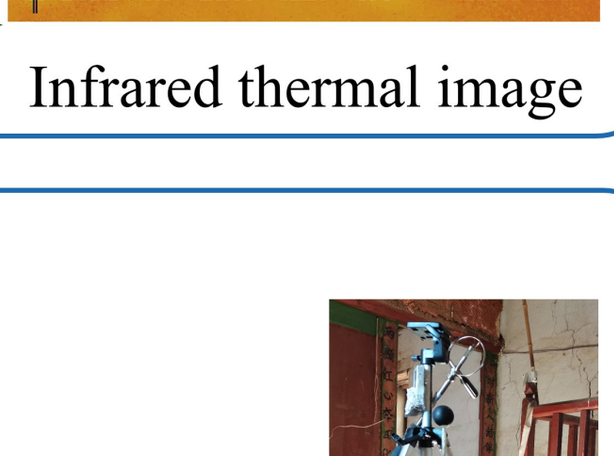

Infrared thermal image

Solar radiation
Perspective
Air temperature
Surface temperature and heat flux
Living room
Bedroom
Bathroom
Courtyard
Storage room

Fig. 4 Measured typical dwellings

Fig. 5 The correlation analysis results between building factors and passive strategies: the building sample was built between 1600 and 1900

Fig. 6 The correlation analysis results between building factors and passive strategies: the building sample was built between 1900 and 2000

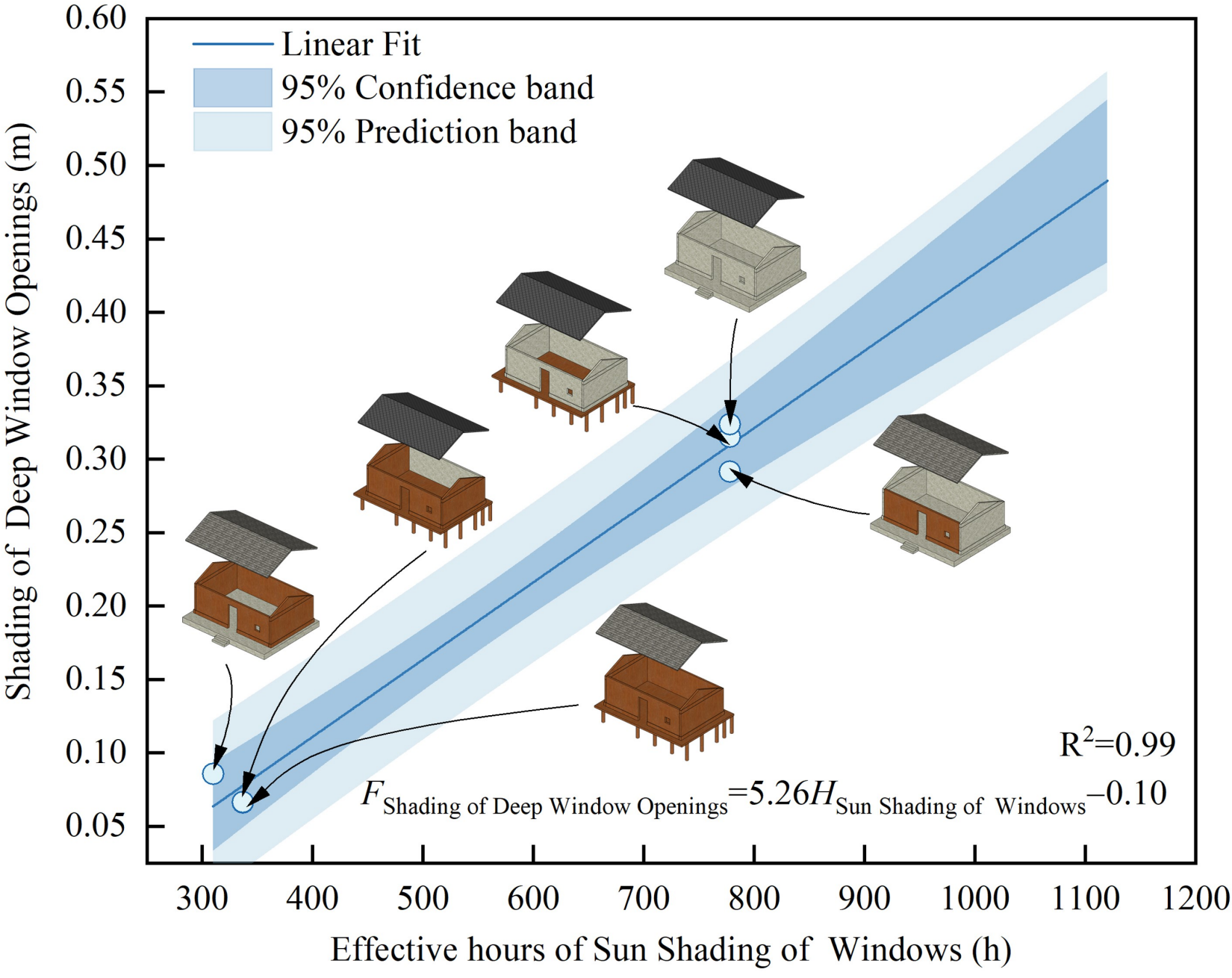

Fig. 7 The linear relationship between Shading of Deep Window Openings and effective hours of Sun Shading of Windows

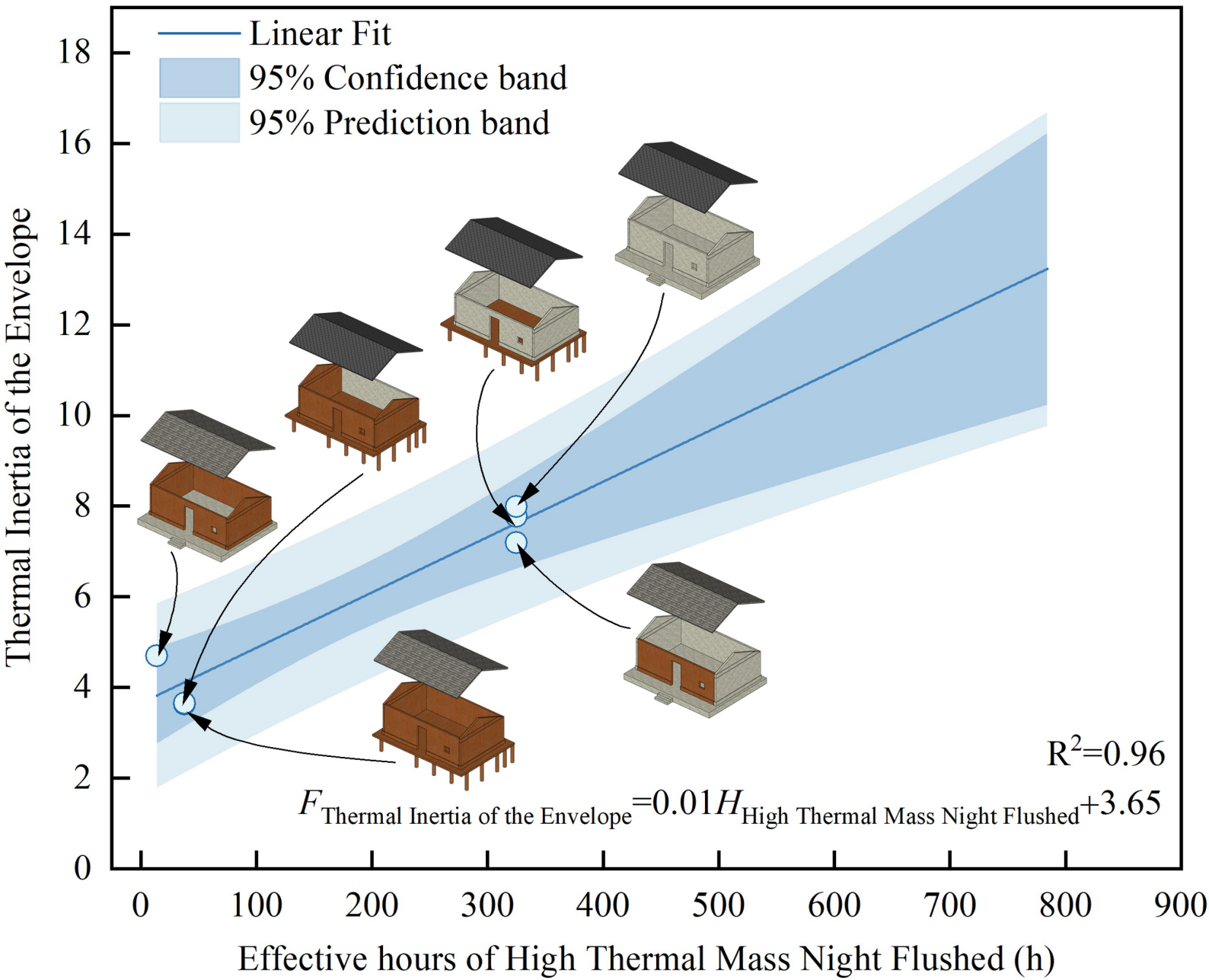

Fig. 8 The linear relationship between the Thermal Inertia of the Envelope and Effective hours of High Thermal Mass Night Flushed

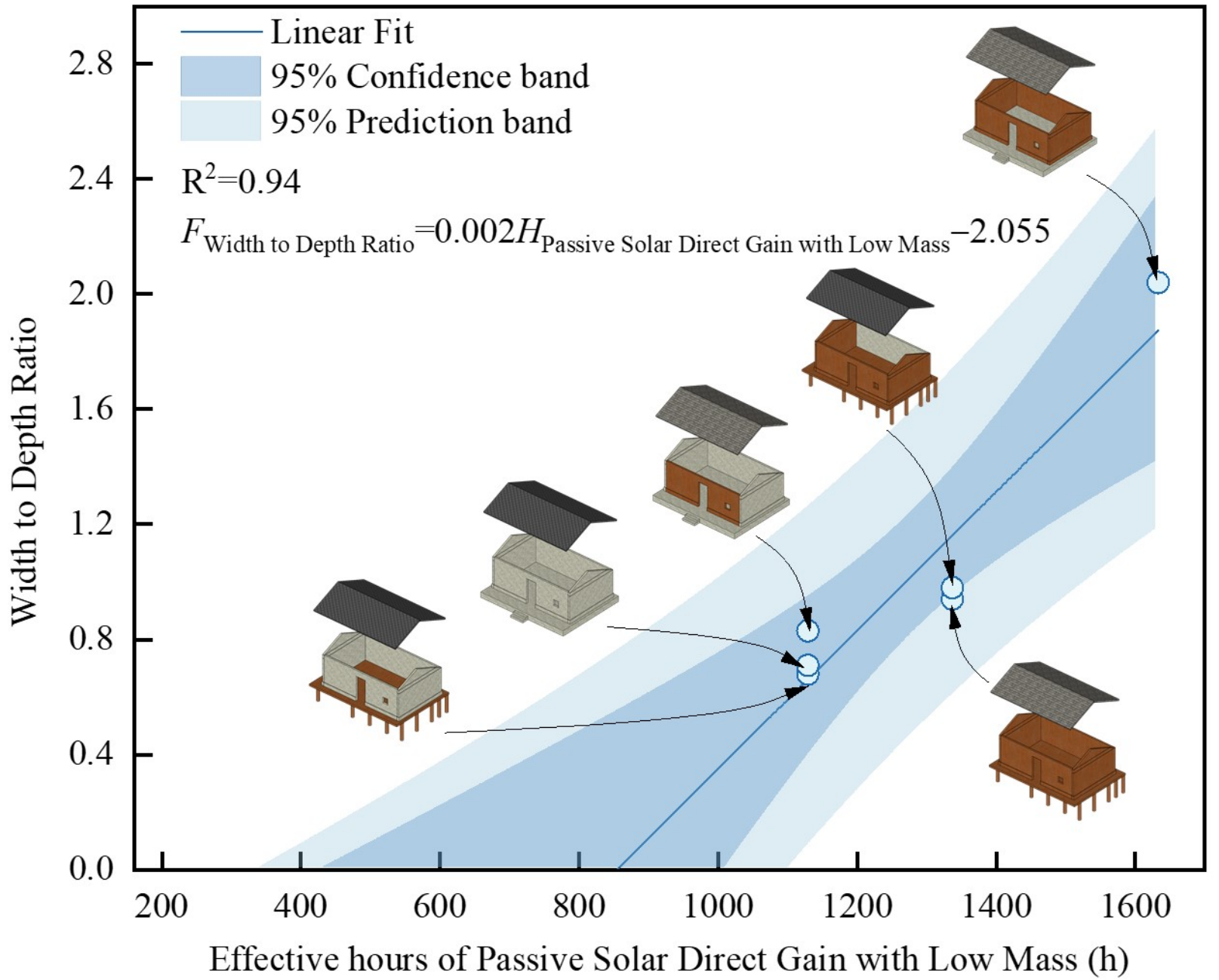

Fig. 9 The linear relationship between Width to Depth Ratio and effective hours of Passive Solar Direct Gain with Low Mass

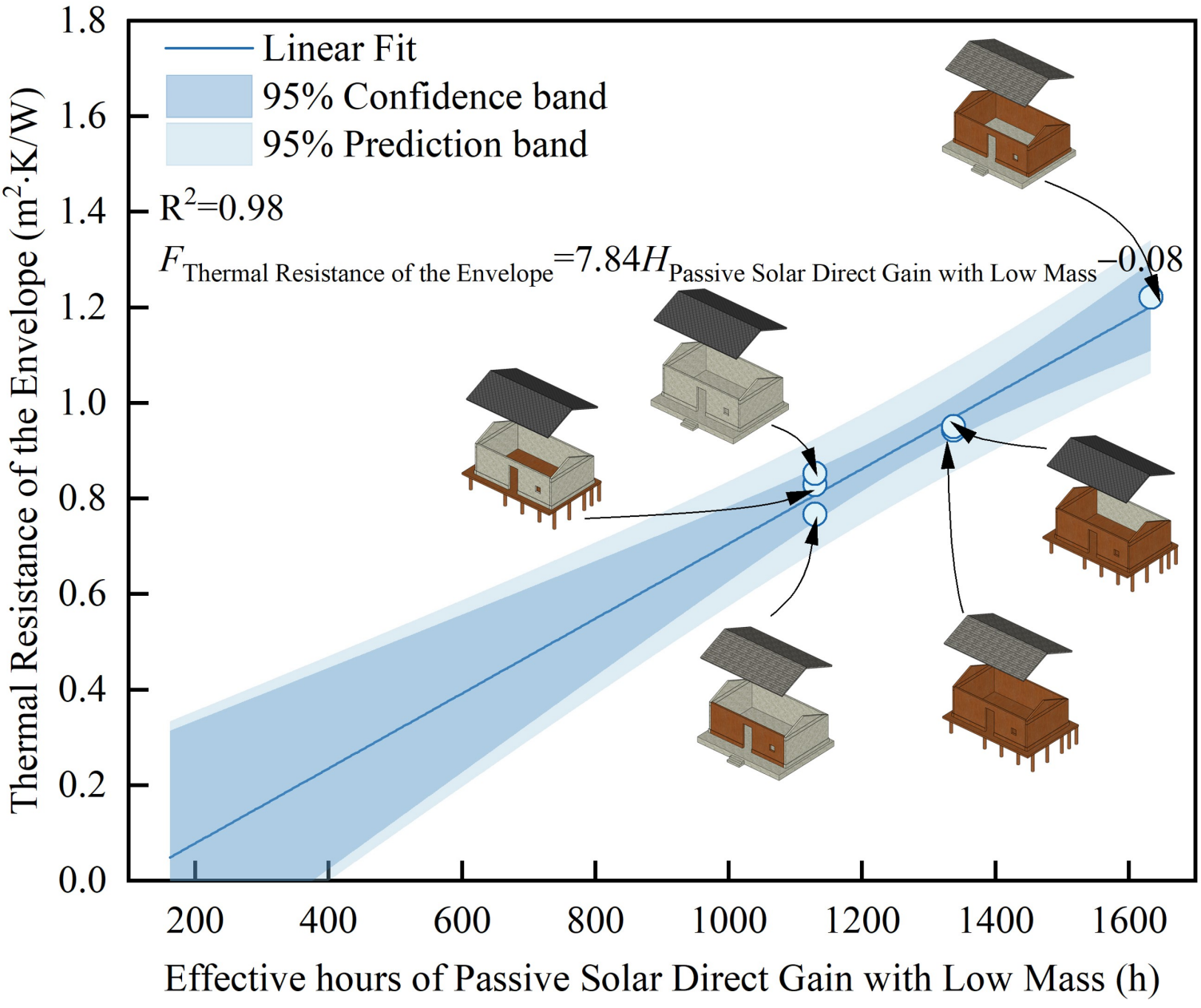

Fig. 10 The linear relationship between the Thermal Resistance of the Envelope and effective hours of Passive Solar Direct Gain with Low Mass

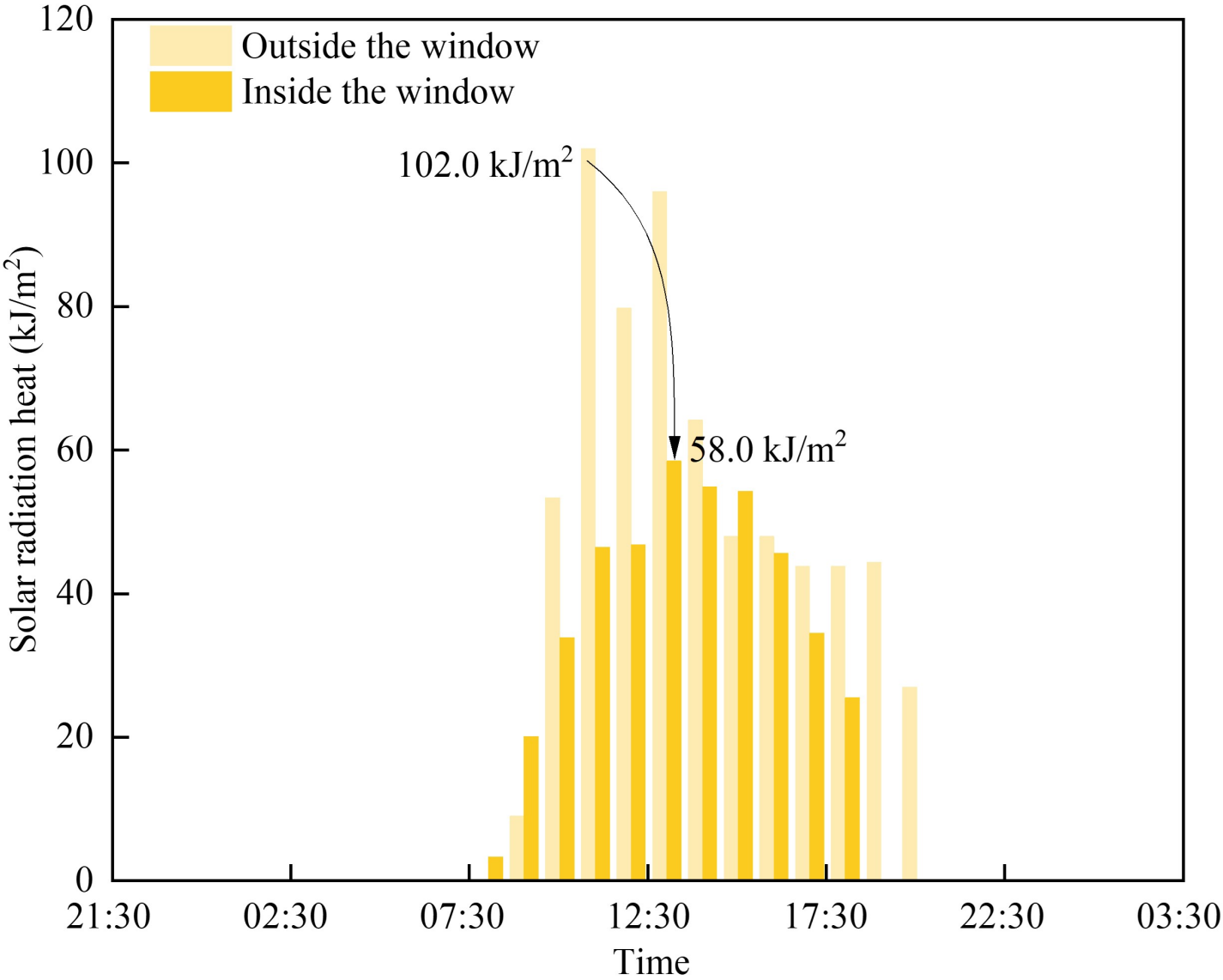

Fig. 11 Heat gain from solar radiation inside and outside the deep window opening in summer

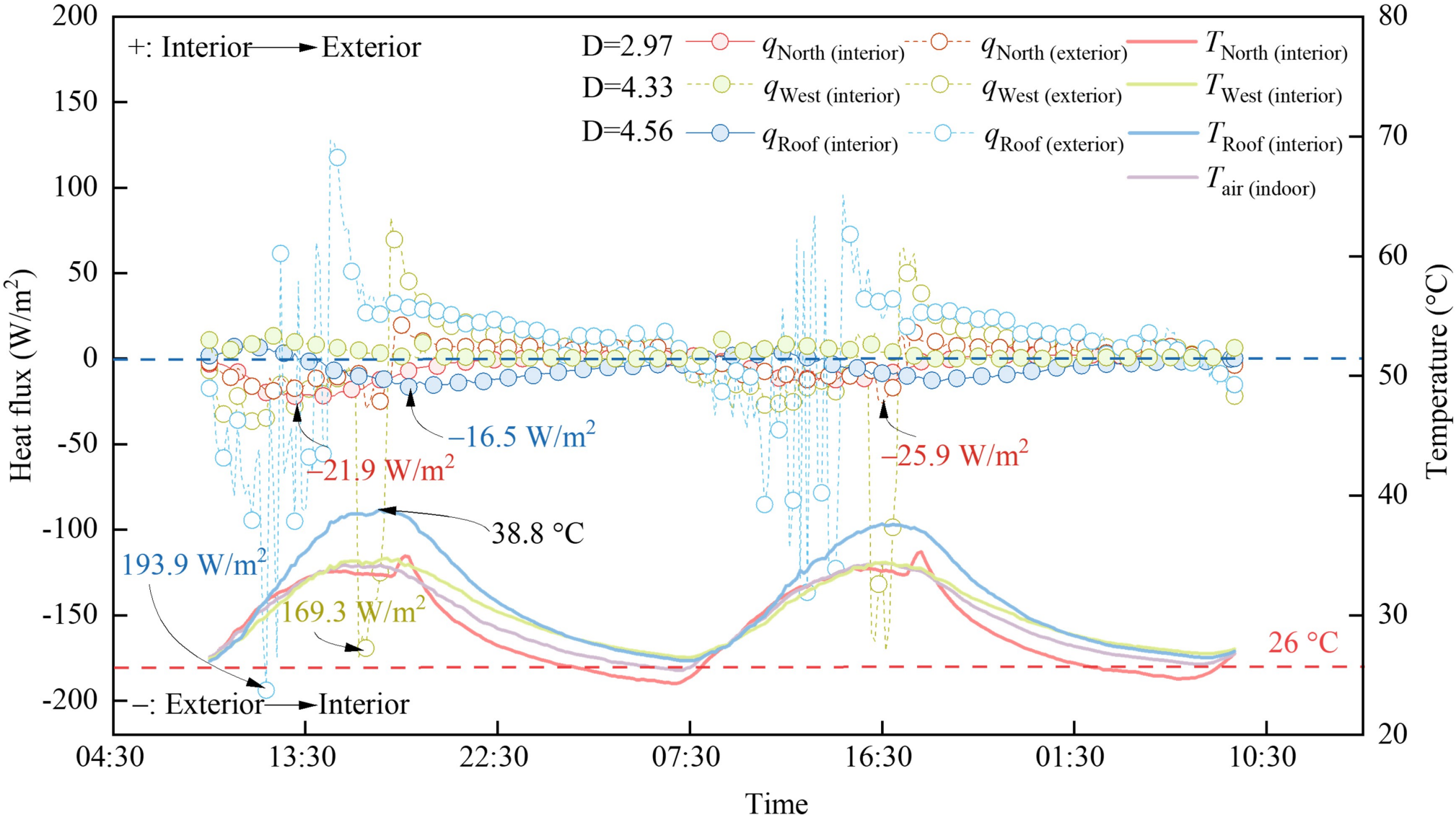

Fig. 12 Surface temperature and heat flux of the envelope in summer

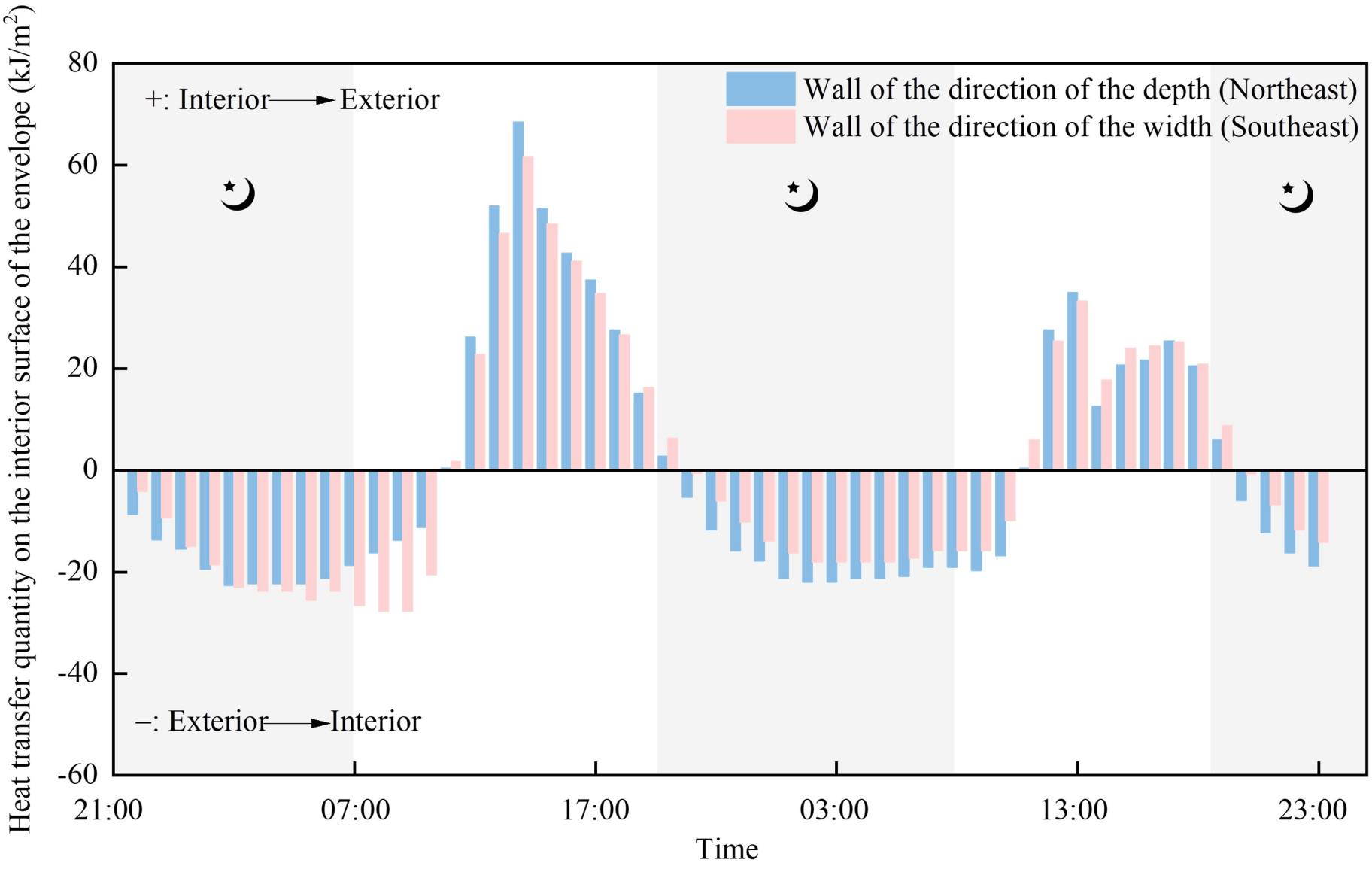

Fig. 13 Heat transfer quantity on the interior surface of walls in the direction of room width and depth in winter

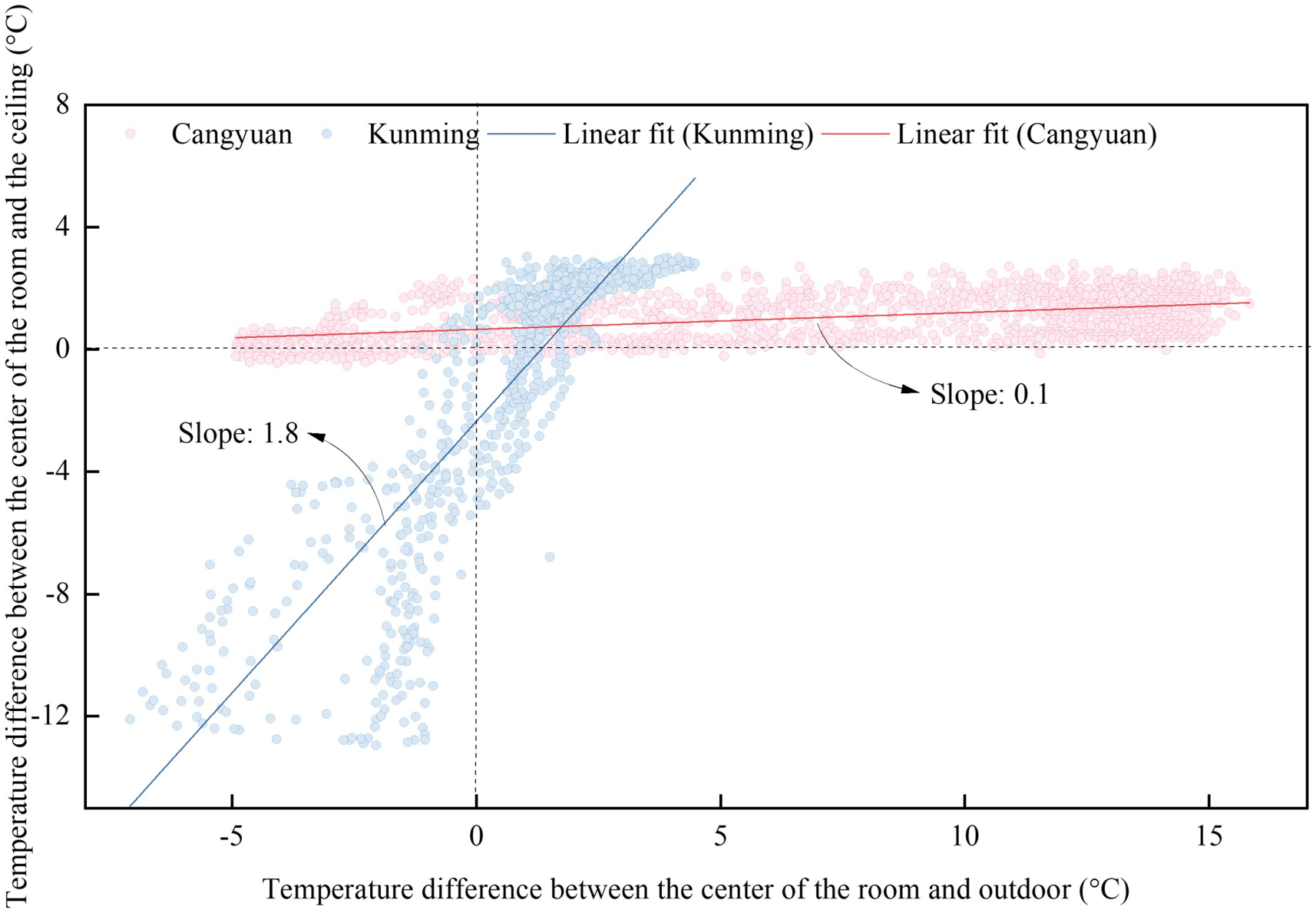

Fig. 14 Relationship between indoor temperature difference at different heights and indoor-outdoor temperature difference